http://www.sciencedirect.com/science/article/pii/S1040618217309448

Middle Bronze Age humidity and temperature variations, and societal changes in East-Central Europe

A. Demény[1], Z. Kern[1], Gy. Czuppon[1], A. Németh[2], G. Schöll-Barna[1], Z. Siklósy[1], Sz. Leél-Őssy[3], G. Cook[4], G. Serlegi[5], B. Bajnóczi[1], P. Sümegi[6], Á. Király[5], V. Kiss[5], G. Kulcsár[5], M. Bondár[5]

[1]*Institute for Geological and Geochemical Research, Research Centre for Astronomy and Earth Sciences, Hungarian Academy of Sciences, H-1112 Budapest, Budaörsi str 45, Hungary, email: demeny@geochem.hu; zoltan.kern@gmail.com; czuppon@geochem.hu; barnagabriella@gmail.com; siklosyzoltan@gmail.com; bajnoczi@geochem.hu,*

[2]*Hertelendi Laboratory of Environmental Studies, Institute for Nuclear Research, MTA, Bem tér, 18/c, H-4026, Debrecen, Hungary, email: nemethalexandra89@gmail.com*

[3]*Department of Physical and Applied Geology, Eötvös Loránd University, Budapest, Pázmány Péter sétány. 1/C, H-1117, Hungary, e-mail: losz@caesar.elte.hu*

[4]*Scottish Universities Environmental Research Centre, Rankine Avenue, Scottish Enterprise Technology Park, East Kilbride, Glasgow G75 0QF, Scotland, UK, e-mail: Gordon.Cook@glasgow.ac.uk*

[5]*Institute of Archaeology, Research Centre for the Humanities, Hungarian Academy of Sciences, H-1019 Budapest, Tóth Kálmán str 4, Hungary; serlegi.gabor@btk.mta.hu; kiraly.agnes@btk.mta.hu; kiss.viktoria@btk.mta.hu; kulcsar.gabriella@btk.mta.hu; bondar@archeo.mta.hu*

[6]*Department of Geology and Paleontology, University of Szeged, H-6722 Szeged, Egyetem str 2, Hungary, sumegi@geo.u-szeged.hu*

Abstract

Archaeological evidence points to substantial changes in Bronze Age societies in the European-Mediterranean region. Isotope geochemical proxies have been compiled to provide independent ancillary data to improve the paleoenvironmental history for the period of interest and support the interpretation of the archaeological observations. In addition to published compositions, in this study we gathered new H isotope data from fluid inclusion hosted water from a stalagmite of the Trió Cave, Southern Hungary, and compared

the H isotope data with existing stable isotope and trace element compositions reported for the stalagmite. Additionally, animal bones and freshwater bivalve shells (*Unio* sp.) were collected from Bronze Age archaeological excavations around Lake Balaton and their stable C and O isotope compositions were measured in order to investigate climate changes and lake evolution processes during this period. The data indicate warm and humid conditions with elevated summer precipitation around 3.7 cal ka BP (Before Present, where present is AD 1950), followed by a short-term deterioration in environmental conditions at about 3.5 cal ka BP. The environment became humid and cold with winter precipitation dominance around 3.5 to 3.4 cal ka BP, then gradually changed to drier conditions at ~3.2 cal ka BP. Significant cultural changes have been inferred for this period on the basis of observations during archaeological excavations. The most straightforward consequences of environmental variations have been found in changes of settlement structure. The paleoclimatological picture is well in line with other East-Central European climate records, indicating that the climate fluctuations took place on a regional scale.

Keywords: Middle Bronze Age; humidity; speleothem; stable isotope compositions; archaeology

1. Introduction

Although the Holocene is a stable climatic period compared to the entire Quaternary, fluctuations have been detected (e.g., Mayewski et al., 2004, Wanner et al., 2011), sometimes inducing major societal changes (e.g., Lamb 1982, Finné et al., 2011, Mensing et al., 2015). In addition to temperature variations, precipitation level and seasonality also play

important roles (e.g., Guiot and Kaniewski, 2015; Peyron et al., 2017), requiring complex interpretation of combined data from independent proxies. In the case of Hungary (East Central Europe), documentary sources provide invaluable contributions to the climate-society interactions over the historical period (Vadas, 2013; Vadas and Rácz, 2013; Kiss and Laszlovszky, 2013; Kiss and Nikolić, 2015). Moreover, changes in Medieval settlement pattern, known from the archaeological evidence in the Great Hungarian Plain, have recently been plausibly linked to long-term hydroclimatological changes using historical and archaeobotanical information (Pinke et al., 2016, 2017). However, the availability of written sources is obviously limited in time (Kiss, 2009). A plethora of archaeological evidence is at hand, suggesting major societal and cultural changes dated to the pre-historical period. The role of independent information deduced from (paleo)environmental proxy records acquire a higher value in determining links between societal changes and climate, because they provide the only means to confirm or refute climate related theories that are established on the basis of fragmentary archaeological information.

One of the most important continental paleoclimate archives are speleothems (cave-hosted carbonate deposits) which can record annual or even seasonal changes in climatic conditions prevailing at the surface above the cave, and preserve this information in the geological record for tens or even hundreds of thousand years (Fairchild and Baker, 2012). Therefore, the speleothem archives have the potential to provide independent information about the environmental conditions of ancient societies. It is apparent that although speleothems are valuable climate recorders, stalagmite formation is a complex system with counteracting factors (Fairchild et al., 2006; Lachniet, 2009) and combined evaluation of different climate proxies is needed to improve the reliability of interpretation. A detailed introduction to speleothem-derived proxy data is beyond the scope of the present study

(see the comprehensive review of Fairchild and Baker, 2012); however, hydrogen isotope analyses of inclusion-hosted water will be introduced briefly because this is a central issue in the current study. Although studies on the stable isotope compositions of water that is trapped in speleothems commenced in the 1970's (Schwarcz et al., 1976; Harmon et al., 1978), relatively few studies have utilized this technique compared to the huge number of investigations using carbon and oxygen isotope data of carbonates. Water-oxygen isotope composition can be recorded by the $\delta^{18}O$ of speleothem calcite, however, this is also influenced by temperature-dependent fractionation, and usually both formation temperature and water composition are unknown parameters. Hydrogen isotope compositions have the advantage that the D/H ratios of the original drip waters are preserved in the fluid inclusions without any fractionation related to precipitation temperature, thus these data record water compositions directly. If the local Meteoric Water Line (a relationship between hydrogen and oxygen isotope compositions of meteoric waters at a given location, e.g. Clark and Fritz, 1997; Fórizs, 2005) is known, the oxygen isotope composition of the drip-water can be calculated from the H isotope data and that, together with calcite composition and the known fractionation relationship, provides the formation temperature (see, for example, Zhang et al., 2008). However, the meteoric water line valid for the drip water may change with time, hence, additional paleoclimatic data are required for firm interpretation of the H and O isotope data.

The present paper deals with the Bronze Age period from 3.9 to 3.2 cal ka BP (Before Present where present is AD 1950) in which significant cultural changes took place in the European-Mediterranean region that could be related to variations in environmental conditions (e.g., Menotti, 2009; Drake, 2012; Meller et al., 2013; Armit et al., 2014; Primavera et al., 2017). Good correlations between C and O isotope compositions of

speleothems from Hungary, Austria and Turkey have been detected (Siklósy et al., 2009), indicating regional abrupt climate changes within this relatively short period. In this study we improved the H isotope record presented by Siklósy et al. (2009) using a stalagmite from the Trió Cave (southern Hungary), producing an age resolution of 30-100 years, to infer temperature and humidity changes. The data are compared with published P and Mg concentration data from the same speleothem (Siklósy et al., 2009) to help the interpretation of the stable isotope data. Another important paleoclimate archive for the region is provided by freshwater bivalves living in Lake Balaton (Schöll-Barna et al., 2012). Shells of freshwater bivalves may provide an appropriate material for paleoenvironmental studies as they reflect the environmental conditions (temperature and humidity) of the warm seasons (e.g., Dettman et al. 1999; Verdegaal et al. 2005; Carroll and Romanek, 2008; Versteegh et al. 2009; Schöne and Fiebig, 2009; Schöll-Barna, 2011). Bivalve shells of *Unio* sp. were collected at archaeological excavation sites at Lake Balaton. The sites were dated by classical pottery typo-chronology, as well as AMS ^{14}C dating of animal bones collected from the same sites. In addition to shell analyses, C and O isotope analyses were also conducted on bone carbonate. Due to constant body temperature, the oxygen isotope composition of the carbonate fraction of the biogenic apatite of animal bones may directly reflect water composition (Longinelli, 1984; Luz and Kolodny, 1985) that in turn is related to ambient temperature (Dansgaard, 1964; Rozanski et al., 1993). On the other hand, C isotope composition of bone carbonate depends on the vegetation type that the animal was fed on. A warmer and drier climate would favour C4 plants with a higher ^{13}C content, whereas in a more humid environment, C3 plants with elevated ^{12}C content would dominate. As a consequence, a change in diet would be reflected in the C isotope composition of the animal's body tissues.

All these climate proxy data were evaluated together that lead to a synthesis of temperature, and humidity and precipitation, as well as seasonality changes in the period of 3.9 to 3.2 cal ka BP. We also explore the effect of these environmental variations on local ancient society.

2. Socio-cultural, economic and ritual transformations in the Pannonian Basin in the Bronze Age

Due to this being an archaeological summary, within this section, the ages are given both as calendar years BP (relative to AD 1950) and in the AD/BC timescale. A summary of Bronze Age archaeological periods and cultures in Hungary is provided in Supplementary Table 1. During the Transitional Period between the Late Copper Age and the beginning of the Early Bronze Age (EBA) in the territory of present-day Hungary (2800/2700–2600/2500 BC; ~4750 to 4450 cal years BP), ceramic styles delineate communication networks covering large areas within the whole Pannonian Basin, with two main groups characterized by the Makó-Kosihy-Čaka and Late Vučedol/Somogyvár-Vinkovci ceramic styles (Bóna, 1992; Bondár, 1996; Kulcsár, 2009; Reményi, 2009; Kulcsár and Szeverényi, 2013). With a few exceptions, the settlement pattern of this phase indicates little social stratification, with little differentiation between the larger centres and the smaller or larger open settlements. In the second half of the EBA (2500/2400–2000/1900 BC; ~ 4450 to 3850 cal years BP), one can observe a transformation that probably grew out of the contact of a southern/Balkan and a northwestern/central European (Bell Beaker) network within the Pannonian Basin. In place of the previous two large stylistic units, new ones covering smaller areas appeared along the Danube and to the east, and developed continuously into the Middle Bronze Age (MBA)

from 2000/1900 BC (~3950 cal years BP) (Bóna, 1992; Neugebauer, 1994; Krenn-Leeb, 2006; Fischl et al., 2013). One of the major features of the MBA is the formation of the so-called 'tell' or stratified settlements that were inhabited for many centuries in the Great Hungarian Plain (Vatya, Hatvan and Füzesabony cultures) (Gogâltan, 2002; O'Shea, 2011; Fischl et al., 2013). However, tell settlements were not found west of this region, while the tells and the fortified hilltop settlements in the central part of Transdanubia seemingly imply the emergence of a new agricultural, economic, political/territorial, social and even ritual system. In the western part of the Pannonian Basin, we encounter the Transdanubian Encrusted Pottery in the MBA (Kiss, 2012). Further to the west, communities belonged to the wider Aunjetitz circle (Gáta/Wieselburg, Unterwölbling) and the southeast Alpine regional groups. All this indicates the emergence of smaller groups that communicated their identities with new, increasingly distinct ceramic styles.

As testified by archaeological findings, the first half of the second millennium BC witnessed major changes in the Pannonian Basin. The classical phase of the MBA ended with a relatively short period of significant transformations, called the Koszider Period (1600-1500/1450 BC; ~3550 to 3450 cal years BP). This latter period corresponds to the last phase of the MBA and represents a transition to the Late Bronze Age (LBA). The transition itself was interpreted by the migration of the mobile pastoralist warriors of the so-called Tumulus culture from the territory of the present-day Southern Germany to the eastern part of Central Europe. Another possible reason for this is the increased intensity of contacts between MBA communities, which may be connected to the widening of regional and interregional exchange networks, through which raw materials and exotic items were acquired, and caused the transformation of identities (Bóna, 1992; Fischl et al., 2013).

Based on the available data, the number and size of settlements increased during the MBA, which probably also indicates demographic growth (Chapman, 1999; Szeverényi, 2004; Kiss, 2012; Fischl et al., 2013). The final phase of the era, the Koszider Period, witnessed a rearrangement of the settled area. However, it is hard to determine whether we can actually observe a settlement nucleation, which would indicate the movement of people into larger 'centres' (Earle and Kolb, 2010; Fischl et al., 2013).

At the beginning of the LBA, the number of settlements in all the above-mentioned regions was lower than in the previous phase. We can detect an overall fall in the number of sites in the Tumulus period, while there are areas that were inhabited for the first time in this phase (V. Szabó, 1999; Sánta, 2010, 2012). The open settlements, with early Tumulus type material that appeared at the end of the MBA, seem to complement the already existing settlement pattern, first in western Transdanubia and in the southern part of the Great Hungarian Plain (Sánta, 2010). Obvious MBA centres like tells and fortified hilltop settlements disappeared and gave way to a network of open settlements throughout Hungary. Settlement patterns without signs of long-term occupation seem to reflect a different social, economic and probably political organization, and a different perspective on the landscape in comparison to the previous centuries (Csányi, 2003; Sánta, 2010; Fischl et al., 2013). Not only settlement structure changed after the Koszider Period. Ceramic styles, metal production, deposition and even burial rites transformed in a way that the overall picture reflects a more heterogeneous society. However, new evidence indicates that the difference between MBA and LBA communities and their subsistence patterns may not be as clear cut as previously suggested. Archaeobotanical and archaeozoological studies do not demonstrate major changes in lifestyle, however, a gradual transition to large livestock herding can be observed (Choyke and Bartosiewicz, 2000; Gyulai, 2010; Vretemark, 2010).

Physical anthropological analysis of skeletal material from some of the cemeteries indicates the continuity of the population, together with an internal restructuring that resulted in a regional anthropological heterogeneity of communities of the Tumulus period (Hajdu, 2012).

The treatment of the corpse also changed over time. In Transdanubia and in the western part of the Great Hungarian Plain, the more or less uniform burial rite of the EBA and MBA communities was cremation. In the eastern and southern parts of the Great Hungarian Plain (among the communities of Füzesabony and Maros styles), inhumation dominated. The MBA graves of females were richly furnished with jewellery while male graves were furnished with weapons, indicating a more stratified society compared to the former period. In the Koszider Period, a larger variety of burial rites occurred and bi-ritual cemeteries became more frequent; however, the practice of providing grave goods continued in the same manner. In the Tumulus period, a new element of circular ditches, with or without a burial mound (tumulus), appeared. The warrior graves of the early and classic Tumulus period, under these mounds, may also indicate stratified societies, however, some cemeteries with uniform burials suggest a more egalitarian society in some territories of the Pannonian Basin (Harding, 2000; Bösel, 2008; Fischl et al., 2013).

By the end of the 15th century BC (~3400 cal years BP), the main European communication network was also reorganized. Instead of the northwest-southeast axis, a north-south oriented channel, which finally bypassed the Pannonian Basin, became dominant. A few centuries later, in the classic and late phases of the LBA, the Danube became a distinct dividing line between western and eastern cultural regions.

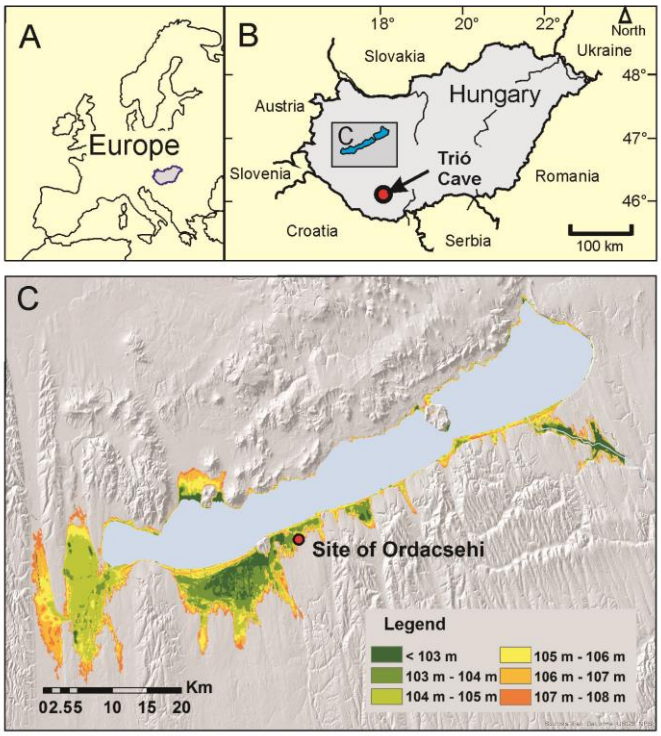

Fig. 1. Locations of the archaeological site of Ordacsehi-Bugaszeg (bivalve shells) and the Trió Cave (stalagmite). Potential lake water levels are shown in C as heights above sea level.

3. Locations and samples

Mollusc shells are frequently found during archaeological excavations along the shoreline of Lake Balaton, presumably as kitchen waste in household rubbish pits. Shells were collected at the site of Ordacsehi-Bugaszeg (Fig. 1) between 2000 and 2002, within the framework of preventive excavations along the M7 highway (Kiss et al, 2007). The site is about 5 km from the present-day shore of the lake, which is the largest shallow lake in Central Europe, with an average depth of 3 m. Due to its shallow depth, it is particularly sensitive to climatic variations. The main processes responsible for lake level variations (apart from recent human activity) are changes in evaporation rate and influx of precipitation, either directly or through rivers and creeks.

Based on archaeological observations, the Ordacsehi-Bugaszeg sites belong to the Bronze Age (about 2.5 to 4.0 cal ka BP), and represent various cultures: Somogyvár-Vinkovci (~4.5-4.2 cal ka BP), Kisapostag (~4.2-3.9 cal ka BP), Late Kisapostag-Early Transdanubian Encrusted Pottery culture (~3.9-3.8 cal ka BP), Transdanubian Encrusted Pottery culture (~3.8-3.6 cal ka BP) and Tumulus culture (~3.6-3.5 cal ka BP) (ages were converted from CE/BCE ages of Visy, 2003 and Fischl et al., 2013).

The Trió Cave (46.7°N, 18.9°E) is located in the western part of the Mecsek Hills, S-Hungary (Fig. 1), at the bottom of the Szuado Valley. The cave is one of the karst systems developed in Anisian Lapis Limestone in the area and comprises ca. 200 m of passages with a catchment area of 3.5 km^2. There is only one artificial entrance, opened in 1969. Corridors blocked by clay and debris were explored and opened from the mid 1990's. The cave is situated in a natural oak and hornbeam forest *(Querco petreae-Carpinetum)*, free from agricultural activities (e.g. ploughing and fertilizing). The host rocks consist of thick (>1000 m) Upper Permian fluvial sandstones, and Triassic shallow marine clastics and carbonates (limestones and dolomites with evaporitic inter-beddings (Nagy, 1968). The general wind direction is westerly to north-westerly and the average annual precipitation in the region is 660 mm. The mean annual temperature within the deep interior of the cave is ca. 10 °C, whereas lower temperatures to ~7°C were found at shallower levels (Muladi et al., 2013). A beehive shaped stalagmite, formed about 30 m from the entrance (where the temperature is about 8 °C, Muladi et al., 2013) , was drilled from the side yielding a core 42 cm in length.

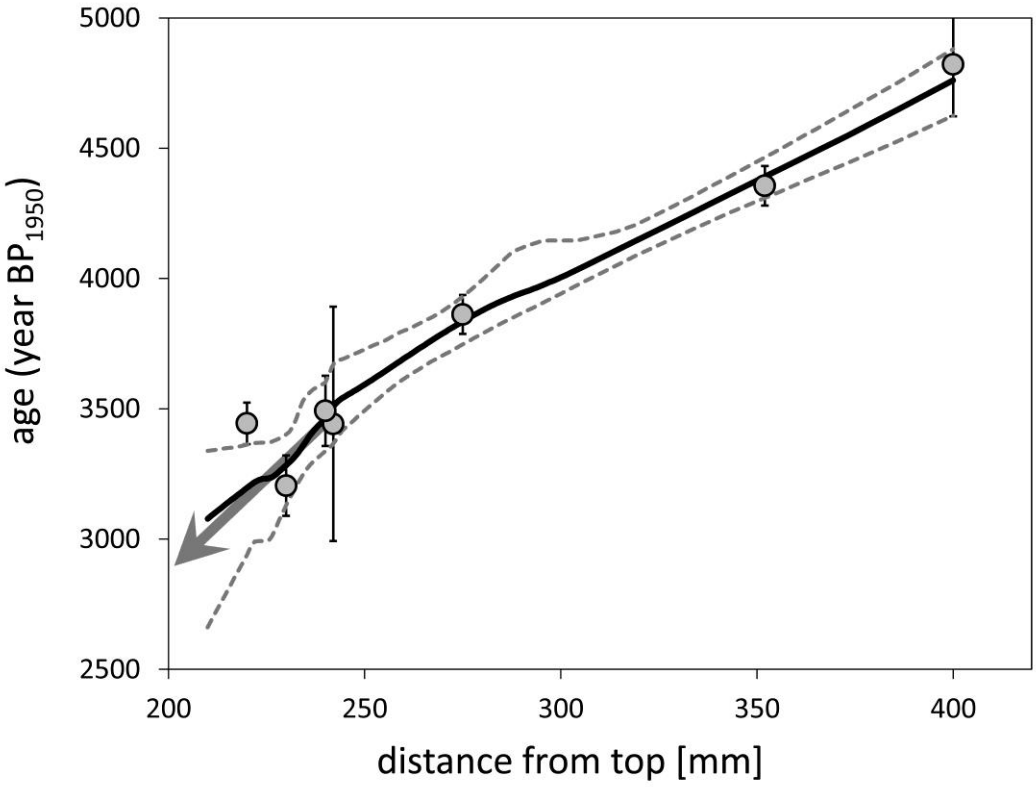

Fig. 2. An age-depth model established from the original U/Th data of Siklósy et al. (2009) using the StalAge algorithm (Scholz and Hoffmann, 2011). The grey arrow marks the direction to the origin.

4. Analytical techniques

Optical microscopic analyses were carried out in crossed-polarised transmission light using a Nikon Eclipse E600 POL optical microscope on polished thin (~100 μm) sections. Results of dating, trace element and stable isotope geochemical analyses, evaluated in this paper, were reported in detail by Siklósy et al. (2009).

4.1. Radiometric age determination

A re-calibrated age-depth model was established from the original U/Th data of Siklósy et al. (2009) using the StalAge algorithm (Scholz and Hoffmann, 2011). In order to

make them comparable with the radiocarbon ages, all U-Th ages are reported as calendar years Before Present (BP) relative to AD 1950. The age-depth model is shown in Fig. 2.

AMS ^{14}C analyses were conducted on bone collagen at the Scottish Universities Environmental Research Centre (SUERC) and at the Vienna Environmental Research Accelerator (VERA) facilities. At SUERC, whole fragments of bone (several mm diameter) were first cleaned by abrading the surface with a Dremel tool fitted with a small buff. The fragments were then placed in cold molar HCl for approximately 2-3 days to effect demineralisation. The acid solution was then decanted and the collagen washed in reverse osmosis water and then placed in further reverse osmosis water. Where necessary, a small amount of 0.5 M HCl was added to adjust the pH of the solution to 3. The solution was then heated gently (to approx. 80°C) for 3-4 hours to dissolve/gelatinise the collagen, cooled, filtered through Whatman GF/A glass fibre paper and freeze dried. 15-20 mg sub-samples were combusted in sealed quartz tubes containing copper oxide and silver foil, according to the method of Vandeputte et al. (1996). All CO_2 samples were extracted under vacuum, cryogenically purified and prepared as graphite targets according to the method of Slota et al. (1987). The $^{14}C/^{13}C$ ratios of the graphitised samples were measured on the SUERC single-stage accelerator mass spectrometer (Freeman et al. 2010), manufactured by National Electrostatics Corporation, Wisconsin and radiocarbon ages calculated using the background subtraction method. Sub-samples of the collagen (approx. 0.7 mg) were analysed for stable carbon isotope ratio using a Thermo-Fisher Delta V Advantage continuous flow isotope ratio mass spectrometer, interfaced to a Costech Instruments elemental analyser system.

The chemical pre-treatment procedure applied at the VERA facility was essentially the same as above; the $^{14}C/^{13}C$ ratios were determined using a tandem AMS system, again built by National Electrostatics Corporation in Wisconsin, USA.

The calibrated ages were calculated using the OxCal4.1 (Bronk Ramsey, 2001) and the INTCAL13-dataset (Reimer et al., 2013).

4.2. Stable isotope geochemistry

Stable H isotope values of fluid inclusion water, and C and O isotope compositions and trace element contents of the calcite from the Trió Cave stalagmite have been reported by Siklósy et al. (2009), thus, the reader is referred to this paper for the analytical procedures. For additional H isotope data, D/H ratios of inclusion-hosted H_2O were determined by vacuum-crushing. Chips of 3-5 mm were placed in stainless steel tubes welded at one end, pumped to vacuum and crushed using a hydraulic press. The released H_2O was purified by vacuum distillation and reacted with Zn at 480 °C to produce H_2 gas (see Demény, 1995, and Demény and Siklósy, 2008). The D/H ratios were determined using a Finnigan MAT delta S mass spectrometer at the Institute for Geological and Geochemical Research, Budapest.

The mineralogy of the shells was checked by cathodoluminescence microscopy (Barbin, 2013) and only those shells preserving the original aragonitic material were used for isotope geochemical analysis (for further details see Schöll-Barna et al., 2012). Aragonite samples from the bivalve shells were collected by drilling equidistantly (with a spatial resolution of about 0.6 mm) on the outer surfaces (pre-cleaned by physically removing the soil-related coating). Bone samples were pre-treated following the procedure suggested by Koch et al. (1997) and Amiot et al. (2010). Samples were powdered and soaked in 2% NaOCl solution for one day to remove organic matter, then treated with 0.1 M acetic acid for one day to remove soil-related carbonate. The samples were rinsed in distilled water 5-10 times after each step. After drying at 50°C, 1, 2 and 3 mg samples were analysed using the same

procedure as for the shell aragonite samples. Stable carbon and oxygen isotope compositions of approximately 150-200 μg carbonate (shell and bone) samples were determined from the carbonate - orthophosphoric acid reaction at 72 °C (Spötl and Vennemann, 2003) and using an automated GASBENCH II sample preparation device attached to a Thermo Finnigan Delta Plus XP mass spectrometer at the Institute for Geological and Geochemical Research, Budapest.

The isotope compositions are expressed in ‰ as δD, $\delta^{13}C$ and $\delta^{18}O$ values relative to V-SMOW (δD values) and V-PDB ($\delta^{13}C$ and $\delta^{18}O$ values), according to the equation: $\delta = (R_{sample}/R_{standard}-1) \times 1000$, where R is the D/H, $^{13}C/^{12}C$ or $^{18}O/^{16}O$ ratio. The measurement precision is better than 0.15‰ for C and O isotope data of carbonates, based on replicate measurements of international standards (NBS-19; NBS-18) and in-house reference materials, and about 3‰ for δD values, based on duplicate analyses. The reproducibility of $\delta^{13}C$ and $\delta^{18}O$ values from measurements on bone carbonates is better than 0.18 and 0.40‰, respectively.

5. Results

5.1. Shells and bones from archaeological excavations

Bones from all five archaeological sites of Ordacsehi-Bugaszeg were dated by AMS ^{14}C, yielding median ages of 3925 to 3539 cal years BP (Table 1, Fig. 3A). Stable carbon and oxygen isotope data of the bivalve shells range from –6.4 to +0.8‰ and –8.6 to –1.7‰, respectively (Table 2). The entire dataset (268 analyses from 10 shells, Supplementary Table 2) yields a positive correlation (R^2=0.62; Fig. 3B), whereas the mean $\delta^{13}C$ and $\delta^{18}O$ values calculated for individual archaeological periods are even better correlated. The $\delta^{13}C$ and

$\delta^{18}O$ data show both within-shell fluctuations (related to seasonal fluctuations reported by Schöll-Barna et al., 2012) and multiannual differences. Plotting the median values of C and O isotope compositions as a function of age (Fig. 3C), the data show a strong fluctuation, with the highest $\delta^{13}C$ and $\delta^{18}O$ values at 3800 cal years BP and very low values at 3670 cal years BP. Stable carbon and oxygen isotope compositions of bone-hosted carbonate range from –13.6 to –10.0‰ and –6.8 to –3.2‰, respectively (Table 2). The $\delta^{13}C_{bone}$ and $\delta^{18}O_{bone}$ patterns are different from each other (Fig. 3D) and from the shell carbonates' isotopic compositions.

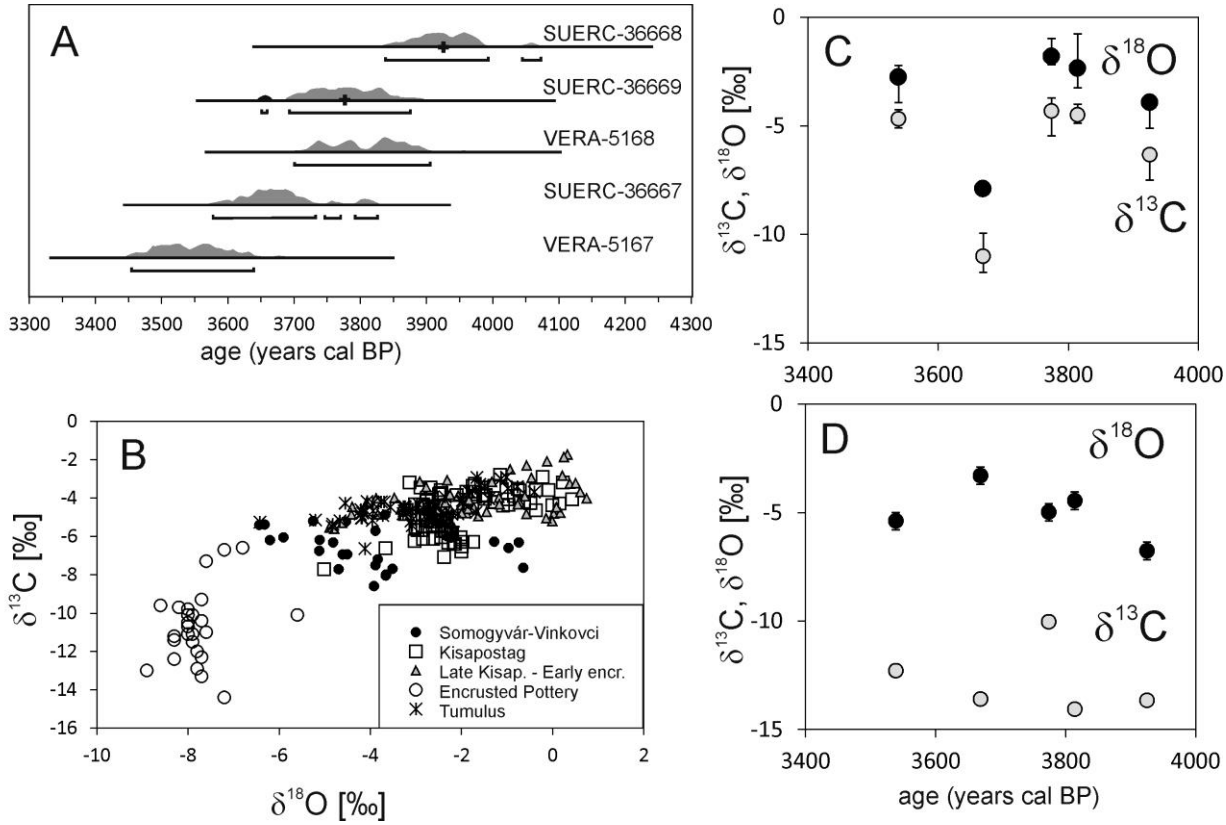

Fig. 3. AMS ^{14}C ages (A) and stable C and O isotope compositions (in ‰ relative to V-PDB) of carbonate contents of Unio sp. shells (B and C) and animal bones (D) collected from archaeological excavation sites of Ordacsehi-Bugaszeg (at Lake Balaton, Western Hungary).

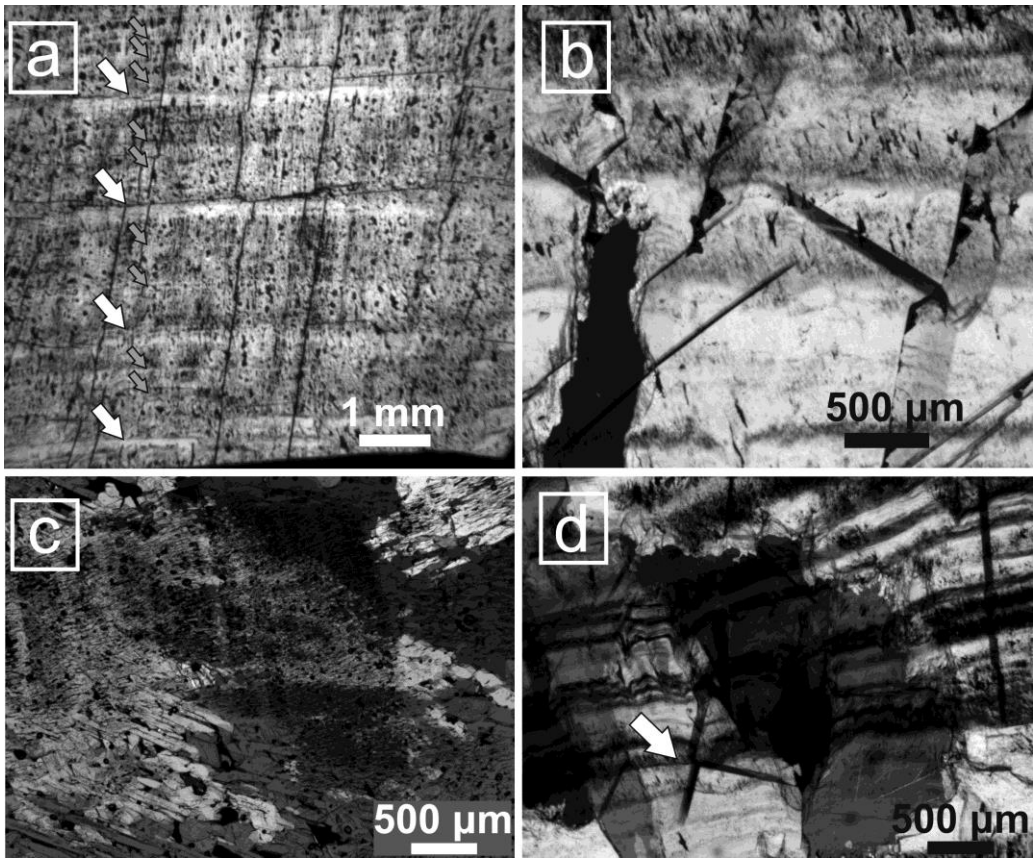

Fig. 4. Carbonate fabrics occurring in the Trió core. (a) Porous columnar fabric with two orders of lamination (sub-laminae connected to thin detrital layers are aligned by blue arrows, while the macroscopically visible compact laminae are aligned by white arrows). (b) Compact columnar fabric with low porosity. (c) Microcrystalline fabric with interfingering extinction boundaries and high porosity. (d) Erosion surface in the lowermost section of the compact columnar fabric aligned by white arrow, covered by a series of brown laminae of detrital origin.

5.2. Petrography of the studied stalagmite section

Four main textural types have been observed in the studied section of the Trió stalagmite (from 200 mm to 360 mm from the top of the core, dft). Microscopic pictures are shown in Fig. 4, while a petrographic log is presented along with stable isotope compositions in Fig. 6 that shows distance intervals cited in the description.

Porous columnar fabric. This is the dominant fabric type in the studied stalagmite section. It is characterized by columnar extinction domains with considerably higher porosity (Fig. 4a). This part of the stalagmite consists of macroscopically white, porous laminae and thinner, translucent, dense laminae. These lamina couplets are relatively thick (1.5-2 mm). Porous laminae are characterized by small, rounded pores, which are organized into 0.1-0.4 mm thick sub-laminae (Fig. 4a, blue arrows) along with thin brown layers of detrital inclusions. Lamination in this fabric is even and parallel. The extinction domains are elongated, have straight boundaries and cut across several laminae, parallel to the direction of growth, similarly described by Boch et al. (2011).

Compact columnar fabric. Macroscopically dark, translucent sections of the core consist of columnar calcite crystals with little or no inter-crystalline porosity (Fig. 4b). Brown laminae of detrital inclusions are common, especially between 250-260 mm dft.

Microcrystalline fabric. This fabric is similar to the open columnar fabric in terms of its lamination of alternating thin compact and thicker porous laminae. However, the extinction domains have serrated interlocking boundaries, crosscutting wide bands of brown micritic/microsparitic laminae. The latter is more typical in the sections between 204-216 and 270-275 mm from the top of the core. Lamination is significantly thinner in these sections (0.1-0.2 mm), while it's the thickest in the section under 310 mm dft (usually thicker than 1 mm), where no brown laminae occur.

Bands of *micrite/microsparite* with high detrital content are observed at narrow intervals that might represent erosional surfaces or highly reduced growth periods. Every lamina is covered by thick brown material (sometimes a series of thin brown laminae can be recognized) along uneven, rounded surfaces (Fig. 4d). One of these surfaces (Fig. 4d, aligned by a white arrow) even cuts into the underlying lamination, which clearly indicates erosion. Lamina couplets have variable thickness.

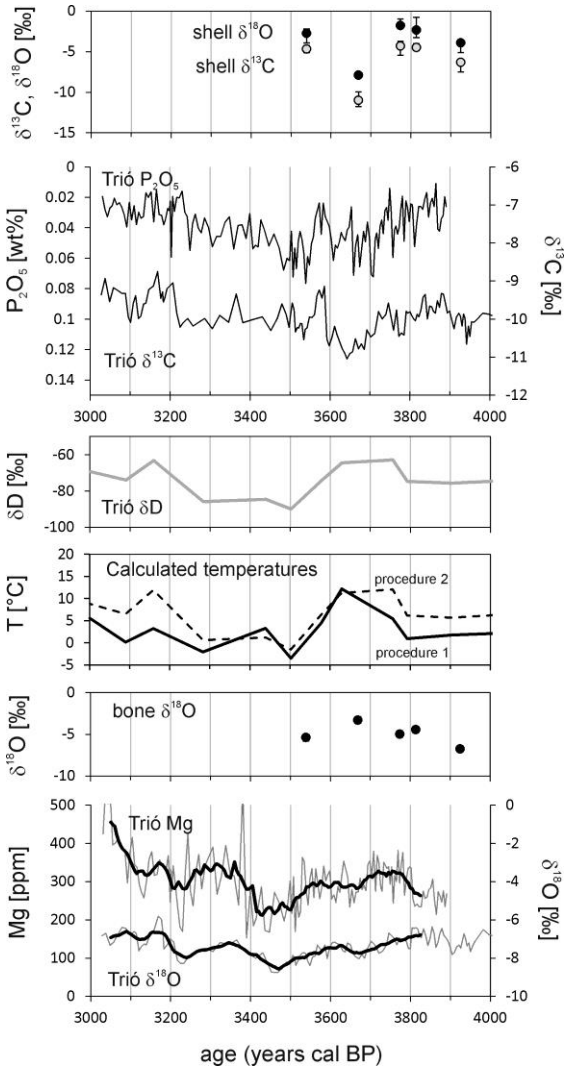

Fig. 5. Stable isotope compositions of shells and bones collected from archaeological excavations, H, C and O isotope compositions inclusion-hosted water and the host calcite along with P and Mg concentrations of the Trió stalagmite (Siklósy et al., 2009). Proxy records are arranged to reflect humidity (shell $\delta^{13}C$ and $\delta^{18}O$, Trió stalagmite P content and and $\delta^{13}C$) and temperature (Trió stalagmite δD, calculated temperatures, bone $\delta^{18}O$, Trió stalagmite Mg contents and $\delta^{18}O$). Calculated temperatures obtained by procedures 1 and 2 (see text) are shown by solid and dashed lines, respectively.

5.3. Geochemical compositions of the Trió stalagmite

The stable C and O isotope and trace element (Mg, P) data, as well as most of the H isotope compositions of the Trió Cave stalagmite, selected for this study, have been published earlier (see supporting material of Siklósy et al., 2009). As the H isotope dataset is supplemented with new analyses, the δD values are listed in Table 2 and shown in Fig. 5, together with the C and O isotope compositions of the host calcite.

P concentrations fluctuate between 50 and 340 ppm, showing an inverse relationship with the $\delta^{13}C$ values (Fig. 5). In order to avoid misalignment of the analytical tracks that were on different pieces of the drill core, the trace element record was tuned to the C isotope record shifted by 30 years, resulting in good match of the positive $\delta^{13}C$ and negative P peaks at 3580 cal years BP. The lowest P concentrations were found around 3.8 and 3.2 cal ka BP, while the period of 3.70 to 3.48 cal ka BP is generally characterized by elevated P content. A short-lived decrease in the P content occurred around 3.6 cal ka BP when a positive $\delta^{13}C$ peak could also be observed (Fig. 5). The Mg concentrations fluctuate between 150 and 550 ppm, showing a positive relationship with the $\delta^{18}O_{calcite}$ values (Fig. 5). In order to quantify the correlation, both records were transformed to temporarily equidistant, with 10-years steps using the PAST program (Hammer et al., 2001). The transformed $\delta^{18}O$ and Mg records are positively correlated with an R value of 0.39 ($p<0.01$), while using 50 year moving average of the transformed records (see Fig. 5) the R value rises to 0.74.

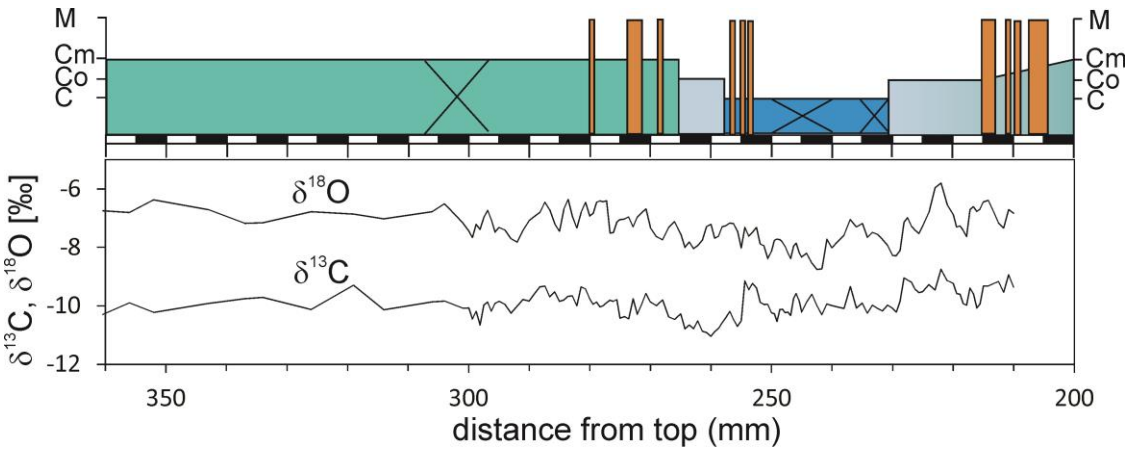

Fig. 6. Microstratigraphic log of the section between 200-360 mm from the top of Trió stalagmite along with stable C and O isotope compositions. Sections not covered with thin sections are marked by X. C: Dense columnar calcite (light blue). Co: porous columnar calcite (dark blue). Cm: Microcrystalline calcite, Ms: micrite/microsparite with high detrital content.

6. Discussion

6.1. Comparison of stable isotope compositions of bones and bivalve shells

Bone carbonate has the advantage, relative to stalagmite calcite, that it forms at constant body temperature and its oxygen isotope composition directly reflects those of the ambient water and food that the animal consumed, provided that the bones preserve their original structural carbonate content and its isotopic composition, and diagenetic carbonate can be eliminated (Lee-Thorp, 2002). Carbon isotope data of bones are not interpreted here as the bone of sample 71/91 derived from a pig, whereas the other samples are from cattle and deer with different diets, and hence different food $\delta^{13}C$ signatures. Since the oxygen isotope composition of meteoric water largely reflects air temperature changes at mid-latitude continental regions (Dansgaard, 1964; Rozanski et al., 1993), elevation in $\delta^{18}O$ values in bone carbonate would indicate higher $\delta^{18}O$ values in the consumed water, which is thought to be coeval with the meteoric water, and consequently, indicate a warmer climate.

These considerations lead to the assumption that the elevated $\delta^{18}O_{bone}$ values (Fig. 3D) might reflect a warmer climate at about 3670 cal years BP.

Mussel shells of the *Unio* sp. were found in the same archaeological excavation sites, most probably buried as waste material from animal feeding. The mussels were collected by the Bronze Age people very likely from Lake Balaton, which is located in the immediate vicinity of the ancient settlements (Fig. 1). A comprehensive study of the C and O isotope compositions of modern shells from the lake found that the isotopic compositions are mainly determined by the lake water budget rather than water temperature (Schöll-Barna et al. 2012). Low lake level caused by intense evaporation during drier periods is associated with elevated $\delta^{13}C$ and $\delta^{18}O$ values in the shells' aragonite, whereas high lake level induced by decreased evaporation and/or increased precipitation and river water input (higher humidity) is reflected by low $\delta^{13}C$ and $\delta^{18}O$ values (Fig. 3).

6.2. Temperature and humidity changes recorded by speleothem-based geochemical proxies

Before stable isotope compositions are interpreted, a short evaluation of petrographic observations and their implications on the stalagmite formation processes is given here.

Porous microcrystalline fabric is the most abundant fabric in the sample, while a truly continuous section of compact columnar fabric can be only found between 230-258 mm dft (Fig. 6). Microcrystalline calcite fabric in stalagmites was observed to form under higher (but variable) discharge than columnar fabric, with larger input of detrital and colloidal particles (Frisia et al., 2000). Seasonally forming porous fabric in lamina couplets was connected to higher cave air temperatures in caves where temperature is related to cave air composition. In Katerloch cave, for example, a more porous columnar fabric formed during summer when

higher cave air temperature resulted in high pCO_2 and low calcite supersaturation in the discharge, which was usually higher while laminae of compact columnar fabric formed during winter (Boch et al., 2011). Similar seasonality in cave air temperature and composition was also observed in Baradla Cave (Demény et al., 2017a) in the north-eastern part of Hungary; therefore, we can assume that the reason behind the alternating compact and more porous lamina couplets in microcrystalline calcite fabric could be the seasonal change in the cave's environmental conditions. From this angle, the compact columnar fabric between 230-258 mm dft (Fig. 6) appears to be an outlier, as its lower section contains erosional surfaces, while the thin and parallel lamination in its upper section is also based on the alternation of compact calcite and thin detrital layers. Compact columnar fabric was associated with lower and more constant drip rates (Frisia and Borsato, 2010), while compact sub-laminae were linked to lower cave air temperatures, resulting in strong ventilation and low pCO_2, which caused higher calcite supersaturation in the discharge. Another example for the connection between a more compact fabric, discharge and its carbonate supersaturation is the observations of Wróblewsky et al. (2017), based on recent flowstones, where more compact fabric precipitated at the season of lower discharge and higher supersaturation.

Columnar and microcrystalline calcite fabrics are considered to be formed under quasi-equilibrium conditions (Frisia and Borsato, 2010), which suggests that although there seems to be a connection between calcite fabric and stable oxygen isotopic composition (Fig. 6), the stable isotope changes are not related to variations in equilibrium and disequilibrium conditions. This is supported by the fact that the $\delta^{13}C$ and $\delta^{18}O$ values of the Trió stalagmite are not correlated.

Carbon and oxygen isotope compositions can be strongly affected by kinetic fractionation in well ventilated caves (Hendy, 1971, Mickler et al., 2004; 2006), producing positive $\delta^{13}C$-$\delta^{18}O$ correlations and obscuring the climate-related signal. Hence, either the presence of kinetic fractionation has to be excluded on the basis of Hendy test analyses (Hendy, 1971), or additional information has to be gathered that supports the climate-related meaning of the $\delta^{13}C$ and $\delta^{18}O$ values (Dorale and Liu, 2009). Since the samples studied in this paper were collected from a drill core, Hendy test analyses along single laminae could not be performed. However, the $\delta^{13}C$ and $\delta^{18}O$ values of the Trió stalagmite are not correlated, suggesting that the kinetic fractionation effect can be considered to be negligible. This statement is also supported by the textural characteristics (see above). Apart from ventilation-related kinetic fractionation, carbon isotope compositions of speleothem carbonate would reflect variations in the relative amount of biogenic CO_2 dissolved from the soil atmosphere and seepage water evolution through carbonate rock dissolution, elevated degree of CO_2 degassing associated with increased evaporation and carbonate precipitation along the solution migration pathway (see Fairchild and Baker, 2012). All of these processes are related to environmental humidity, as a higher amount of precipitation would i) promote soil activity producing more organic-derived CO_2, ii) induce shorter residence times of seepage water in fractures and consequently changes in host rock dissolution and iii) fill up the fracture system with water. The decrease in the air filled void volume in the karstic system during high precipitation periods would decrease the degree of ventilation and hence evaporation efficiency, both in the fracture system and in the cave. A complete understanding of the behaviour of the karstic system would require detailed monitoring, including ^{14}C activity measurements from a soil zone to the drip waters (Fohlmeister et al., 2010). That was not possible due to the strict protection of the Trió Cave. In the absence of

such data, the relative contribution of host rock-derived carbon to biogenic (from soil respiration and decomposition of old organic matter) and atmospheric carbon (Fohlmeister et al., 2010; Griffiths et al., 2012; Noronha et al., 2014) is difficult to estimate. In order to determine the dominating process that governed $\delta^{13}C$ changes in the Trió speleothem, additional humidity proxies are needed that would not depend on host rock dissolution and ventilation-related fractionation processes.

Such information on humidity changes can be found in the P concentration record. In general, higher P concentrations during more humid periods are consistent with the role of P as a nutrient element in soil biological activity (Huang et al., 2001; Fairchild et al., 2001), and hence its concentration in speleothems may be considered as a proxy for surface bio-productivity (Treble et al., 2003). For a complete understanding, the entire soil and karst system should be monitored in order to determine the mechanisms of seasonal P mobilization, transport and incorporation into the speleothem structure (Borsato et al., 2007), which would exceed the scope of this paper. In the absence of such detailed monitoring data, the coupled P and $\delta^{13}C$ changes (Fig. 5) can be used to infer that $\delta^{13}C$ can reflect past humidity fluctuations (Regattieri et al., 2016).

The entire stalagmite record starts at about 4.7 cal ka BP, while the period of 3.9 to 3.2 cal ka BP was analysed at high resolution (0.5-1 mm, corresponding to 1-30 years, depending on growth rate). At ~ 3.9 cal ka BP, the $\delta^{13}C$ values show a negative shift (Fig. 5), indicating a short-term humid phase. At about 3.8 cal ka BP, the $\delta^{13}C$ values are elevated, suggesting a relatively arid climate that continuously changes to higher humidity, reaching a $\delta^{13}C$ minimum at ~3.65 cal ka BP. After the negative $\delta^{13}C$ peak, the data indicate decreasing precipitation with strong $\delta^{13}C$ fluctuations. A prominent positive $\delta^{13}C$ peak appears at 3.58 cal ka BP that was interpreted as a sign of soil activity decrease due to deposition of volcanic

material (Siklósy et al., 2009). The most arid conditions can be expected at ~3.2 cal ka BP when $\delta^{13}C$ reached its highest values.

An independent view on precipitation level is provided by the stable isotope compositions of mussel shells (Fig. 5). According to Schöll-Barna et al. (2012), the elevated $\delta^{13}C$ and $\delta^{18}O$ values in the mussel shell carbonate would correspond to more arid conditions at about 3.8 cal ka BP, and the strong negative isotope shifts between ~3.7 and 3.6 cal ka BP would indicate more humid conditions. The shell data reflect changes in the speleothem $\delta^{13}C$ record that starts with a short-term humid peak at 3.9 ka followed by an ~1 ‰ rise and a strong decrease between 3.7 and 3.6 cal ka BP. The shell $\delta^{13}C$ and $\delta^{18}O$ data independently support the assumption that the speleothem $\delta^{13}C$ and P records reflect humidity changes, with more arid conditions around 3.8 cal ka BP and a humid peak at about 3.7-3.6 cal ka BP.

Stable oxygen isotope composition of speleothem calcite is basically determined by formation temperature and water composition, expressed by the temperature-dependent calcite-water fractionation relationship (O'Neil et al., 1969). Further, the drip water composition is a result of the combined effects of different processes acting in the atmosphere and in the karstic system (Lachniet, 2009). Moisture origin, transport trajectory, rainfall level, evaporation, seasonal variations (relative amounts of cold and warm seasons' precipitation), infiltration, migration routes and mixing in the karstic system, as well as evaporation in the rock fractures and cave caverns all affect the $\delta^{18}O$ value of the drip water (Lachniet, 2009). Additionally, the $\delta^{18}O$ values of precipitation water (and hence drip water) depend on atmospheric temperature, with a gradient of about 0.3 ‰°C^{-1} in mountainous areas of Hungary (see Demény et al., 2017b), causing ^{18}O-enrichment in the drip water with elevated temperature. The temperature-dependent calcite-water oxygen isotope

fractionation gradient is –0.24 ‰ °C^{-1} (O'Neil et al., 1969). As a result, the net effect is a slight positive relationship between $\delta^{18}O$ values of the precipitated calcite and formation temperature. However, the effects described above show that although the $\delta^{18}O_{calcite}$ values are basically indicating temperature changes, the variations may not be easy to interpret without additional information.

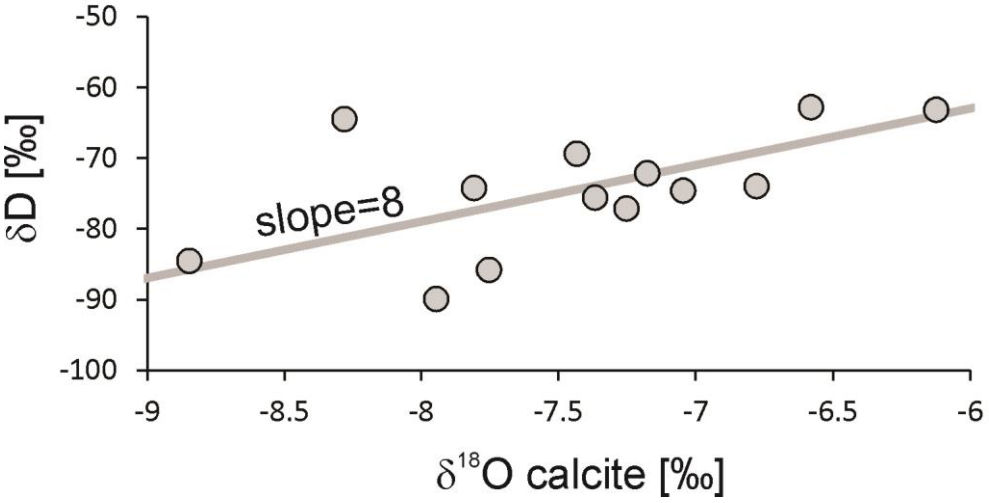

Fig. 7. Stable hydrogen isotope compositions (relative to V-SMOW) of inclusion-hosted water and oxygen isotope compositions of the host calcite (relative to V-PDB) at the inclusion sampling intervals of the Trió stalagmite. The grey line (arbitrarily placed within the sample points) marks slope=8 characteristic for the Global Meteoric Water Line (Craig, 1961).

An independent view on drip water composition is provided by H isotope analyses of inclusion-hosted water. The δD values show a positive correlation with the $\delta^{18}O$ values of the host calcite that match a line with a slope of 8 (Fig. 7). If the host calcite's oxygen isotope composition reflects the drip water composition as described above, then the local meteoric water line's slope (about 7.9, Fórizs et al., 2013) would be transferred to the δD-$\delta^{18}O_{calcite}$ correlation, as observed in Fig. 7. This gives credit to the assumption that the Trió speleothem's $\delta^{18}O$ record reflects temperature changes.

The δD and the $\delta^{18}O_{calcite}$ values together can be used to estimate formation temperatures. Calculation of formation temperature was conducted following two concepts based on measured hydrogen isotope compositions of inclusion-hosted water.

Procedure 1. The steps of the procedure of Zhang et al. (2008) are the following:

1) The oxygen isotope composition of water ($\delta^{18}O_w$) is calculated from the δD data using the linear relation ($\delta D=7.9\cdot\delta^{18}O+11.1$) determined for spring waters of the Mecsek karstic region (Koltai et al. 2013).

2) Mean oxygen isotope compositions for calcites of the 3-5 mm sampling spots of H isotope analyses are gathered from the higher resolution data of Siklósy et al. (2009).

3) Oxygen isotope fractionation values between calcite and water can be calculated using the equation: $\alpha = (1000+\delta^{18}O_{calcite})/(1000+\delta^{18}O_{water})$.

4) Then formation temperature is calculated using the relationship between calcite-water oxygen isotope fractionation and temperature. The empirical equation $1000\cdot\ln\alpha=17.66\cdot(1000/T)-30.16$, where T is temperature in K (Johnston et al., 2013), is used. Note here that this paper also included the earlier data from both popular and frequently cited seminal papers (Coplen, 2007 and Tremaine et al., 2011) and reported new ones, resulting in a presumably more robust equation based on a more extensive dataset. Although it is worth mentioning, that for a calcite precipitated in specific cave environment, the potentially important factors may not be all recognized, hence it is difficult to choose a specific equation. For a detailed discussion on the effect of the governing factors (temperature, pH, growth rate, degassing and drip rate effects) on calcite-water isotope fractionation, see Watkins et al. (2014).

Procedure 2. The procedure used by Demény et al. (2017b) is based on the measured δD values and the relationship between δD and air temperature (δD-T gradient). The steps in the procedure are the following:

1) The differences between the δD values of inclusion water and the present-day drip water δD (~–67 ±2 ‰, 7 occasional sampling from February to June, 2014, Gy. Czuppon, unpublished data) are calculated.

2) The δD differences are divided by the δD-T gradient (the relationship between precipitation H isotope composition and atmospheric temperature) that gives the difference between the past and the present-day temperatures. A preliminary monitoring study of the local precipitation's stable isotope composition (from January 2013 to November 2016, monthly sampling, n=45, Gy. Czuppon, unpublished results) yielded a δD-T gradient of 2.0 ‰°C^{-1}. It is interesting to note that the gradient is very close to the value of 2.1 ‰°C^{-1} determined by Demény et al. (2017b) for a cave in a similar environment and about 200 km to the north (Baradla Cave). The present-day drip water composition of the Baradla Cave (–64.6 ±1.4 ‰, Czuppon et al., 2017) is also close to the Trió compositions (δD=–67 ‰), which gives credit to the use of the δD-T gradient.

3) Finally, the temperature differences are added to the present-day annual mean temperature (~10 °C, Muladi et al., 2013) to yield the past multiannual mean air temperature.

The temperatures obtained by applying these two procedures are plotted in Fig. 5. The results provided using the δD-T gradient (procedure 2) are either very close or higher than those yielded by the coupled δD-$\delta^{18}O_{carb}$ calculations (procedure 1). The former results are closer to present-day cave temperatures (7 to 10 °C from surface entrance to a deep chamber, Muladi et al., 2013), but the warmer-than-present temperatures at 3.7-3.8 cal ka

BP and the very cold conditions at 3.3-3.6 cal ka BP are reproduced in both calculations. The mean difference between the curves from procedure 2 and procedure 1 is 3.6 °C, which is close to the ~3 °C difference between the deep chambers and the sites close to the cave entrance (Muladi et al., 2013). As procedure 1 corresponds to formation temperature (about 8 °C at the present sampling site), while procedure 2 yields annual mean atmospheric temperature (about 10 °C), the observed difference may be meaningful, but calculation uncertainties should be taken into account.

The calculations using the concept of Zhang et al. (2008) are affected by uncertainties in the meteoric water line equation, the selected calcite-water oxygen isotope fractionation equation and the analytical errors for the isotope analyses. Using the Global Meteoric Water line equation ($\delta D=8\cdot\delta^{18}O+10$; Craig, 1961) instead of the karstic water line of Koltai et al. (2013), and substituting 0.2 and 3‰ analytical errors for $\delta^{18}O_{calcite}$ and δD values, respectively, a maximum uncertainty of about 3.6 °C was obtained (based on a worst case scenario with both analytical errors acting in the same direction, which is unlikely), which is close to the difference between the results of the two procedures.

Opposite to the former method that suffers from several unknown variables, the uncertainties of the calculation using the δD-T gradient depend only on the analytical precision and the potential changes in the reference water composition, and the gradient value with time. Despite these differences, the δD-T gradient-based calculation yielded a similar pattern to the Zhang et al. (2008) procedure's results. Taking the relatively stable conditions within the Holocene into account, the temperatures around 12 °C are difficult to explain with atmospheric warming producing a 2°C rise in annual average temperature. However, increasing the reference δD value from –67 to –63 ‰ would shift the calculated temperatures by 2°C. This means that a slight increase in the relative contribution of

summer (D-enriched) precipitation in the infiltrated water or evaporation along the infiltration and the percolation route (D-enrichment during drier period) can easily explain the calculated - and hence in this case virtual - temperature rise. On the other hand, changing the reference δD value to –80 °C would bring the calculated temperatures of the 3.55-3.3 cal ka BP period to present-day values. Such low δD values are generally measured during the winter months, as determined for the Baradla Cave system (Demény et al., 2017b) and for the Trió cave's area, by the preliminary monitoring of Gy. Czuppon (for December-January-February of 2013-2016, δD= –85 ±16 ‰). This suggests an increased contribution of winter precipitation to the percolating karstic water during the period of 3.55 to 3.3 cal ka BP.

Although not fully independent, as they both used the δD values as an input parameter, the similarities in the temperature patterns obtained by the two methods support each other. The above considerations indicate that the temperature calculations would not only yield information on warming and cooling, but seasonality variations may also be inferred from the results. The required seasonality changes would correspond to extreme conditions, the real environmental conditions were most probably characterized by coupled warming + a summer precipitation increase, and cooling + a winter precipitation increase.

Another important geochemical dataset is the Mg concentration record (Fig. 5). Similar to the stable isotope data, Mg concentrations in the drip water and the speleothem carbonate are affected by numerous processes: rock dissolution during water migration, prior calcite precipitation in the fractures and voids, evaporation, mixing of karstic water systems, and temperature-dependent partitioning between drip water and carbonate (see Fairchild and Baker, 2012). Most of these effects are related to humidity as a lower amount

of meteoric precipitation and decreased water infiltration would increase the effect of evaporation and the water residence time in the karstic system, resulting in an elevated Mg content in the drip water and consequently in the speleothem, during drier periods (Huang et al., 2001). Additionally, strong evaporation in the water migration pathway induces prior calcite precipitation in the rock fractures that can also cause Mg enrichment in the drip water (Borsato, et al., 2016). However, the pattern of Mg concentration follows the $\delta^{18}O$ variation (Fig. 5), indicating a common mechanism behind these changes. Interestingly, the temperature calculations yielded warm conditions at ~3.8-3.7 and ~3.2-3.1 cal ka BP when Mg concentrations are high and cold conditions around 3.5 cal ka BP when the Mg concentrations reached a minimum. A positive Mg-T relationship has been experimentally determined by Huang and Fairchild (2001), although the effect of calcite-solution partitioning cannot explain the ~200 ppm Mg content fluctuations observed here. This indicates that additional (e.g., humidity-related) factors may also have affected the Mg concentrations. At higher(lower) ambient temperatures the degree of evapotranspiration is also higher(lower), leading to reduced(increased) infiltration and increased(decreased) trace element contents and $\delta^{18}O$ values in the percolating water. The long-term similarity in the $\delta^{13}C$, $\delta^{18}O$, Mg and P patterns (higher $\delta^{13}C$-$\delta^{18}O$-Mg and lower P values at ~3.8 and 3.2 ka BP and lower $\delta^{13}C$-$\delta^{18}O$-Mg values with higher P concentrations between these periods, Fig. 5) suggests that coupled changes in temperature and soil aridity affected these variables, but the short-term differences (e.g., $\delta^{13}C$ minimum at 3.65 ka BP and $\delta^{18}O$ minimum at 3.47 cal ka BP) indicate that precipitation amount and temperature changes were independent in a centennial scale. However, the good fit of calculated temperature data, the Mg and $\delta^{18}O$ variations and the expected calcite-solution Mg partitioning indicates that these records reflect real temperature variations.

As we have seen, temperature fluctuations may be recorded by the bone $\delta^{18}O$ values that have their maximum at ~3.7 ka, when the highest temperature was obtained from the δD values and when the speleothem $\delta^{18}O$ values and Mg concentrations are high (Fig. 5). The changes in bone composition indicate that the both the δD data and the $\delta^{18}O$-Mg records reflect temperature variations.

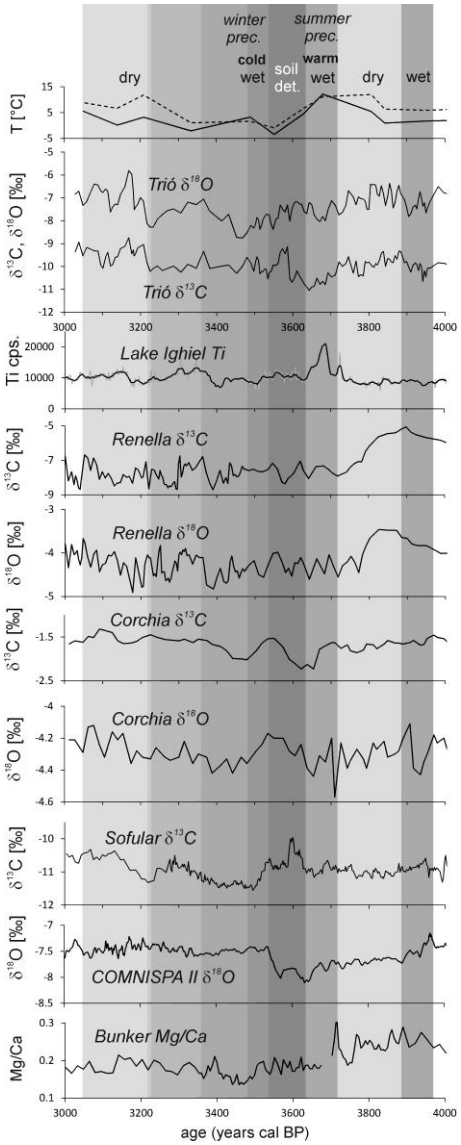

Fig. 8. Temperature and precipitation proxy records for the Trió cave stalagmite (this study) and regional records. Data sources: Corchia cave (northern Italy): Regattieri et al. (2014); Renella cave (northern Italy): Zanchetta et al. (2016); Sofular Cave (northern Turkey): Fleitmann et al. (2009); Spannagel Cave (Austria): Fohlmeister et al. (2013); Bunker Cave (Germany): Fohlmeister et al. (2012); Lake Ighiel (Romania): Haliuc et al. (2017). Dark grey bars indicate humid phases, light grey bars mark dry periods.

6.3. Comparison with regional records

Speleothem-based temperature and/or humidity proxy records that cover the period from 4 to 3 cal ka BP at a temporal resolution comparable with the Trió stalagmite record (~8 years) are rather scarce in Europe. For the Mediterranean region, stable isotope and trace element records from the Corchia and Renella caves (Northern Italy, Regattieri et al., 2014; Zanchetta et al., 2016) are available for the period of 4 to 3 cal ka BP with average temporal resolutions of 16 and 11 years. The records of Drysdale et al. (2006) and Frisia et al. (2005) were not included here due to the relatively low temporal resolution (~60 and 80 years, respectively). The $\delta^{13}C$ record from the Sofular Cave (stalagmite SO-1), northern Turkey (Fleitmann et al., 2009) was selected due to the highly precise ages and the high resolution of the isotope record (~3 years on average). Although the precipitation level and moisture transport information provided by the SO-1 record is representative mainly for the Black Sea region (Fleitmann et al., 2009), the atmospheric teleconnections (Türkes and Erlat, 2003) indicate that the isotope patterns may be compared with European records.

In central Europe, speleothems from the Spannagel Cave provided highly resolved (~1.5 years) $\delta^{18}O$ data (the COMNISPA II record, Fohlmeister et al., 2013) that can be compared with the data presented in this paper. The composite oxygen isotope record of five stalagmites collected in the Spannagel Cave, Austria (COMNISPA II) has been interpreted as a proxy for winter precipitation level and temperature variations, related to the North Atlantic Oscillation (Mangini et al., 2007; Fohlmeister et al., 2013). Further to the north-western part of Europe, Mg/Ca data from the BU-4 stalagmite of the Bunker Cave, Germany (Fohlmeister et al., 2012) reflect humidity changes with low Mg/Ca values corresponding to elevated precipitation levels and vice versa (temporal resolution: ~8 years).

Although not related to speleothem research, a lake sediment record from the Trascău Mts (Lake Ighiel, Romania) is included in the discussion due to its well-constrained age-depth model and the high (~annual) resolution of the geochemical record obtained by an XRF scanner (Haliuc et al., 2017). The Ti counts in the Lake Ighiel sequence are interpreted as a proxy for runoff events by Haliuc et al. (2017).

The records obtained in the present study and selected from the literature are compiled in a composite figure (Fig. 8), whose complex interpretation and a synthesis follows below.

The period between 3.9 and 3.7 cal ka BP starts with a peak representing a period of high humidity, recorded by the $\delta^{13}C$ records of the Trió Cave and the mussel shell remnants that changes to drier conditions on the base of elevated dc that changes to drier conditions on the base of elevated $\delta^{13}C$ values of both carbonate types (Fig. 5). The high isotope values of the Trió and the Renella stalagmites and the elevated Mg/Ca data of the Bunker Cave stalagmite around 3.8 ka (Fig. 8) indicate a relatively dry environment in eastern and western Central Europe that ends with an abrupt change to very humid conditions at 3.7 ka. The event-like character of this humid phase is shown by the negative $\delta^{13}C$ peak and the P concentration increase in the Trió stalagmite, the strong negative $\delta^{13}C$ and $\delta^{18}O$ shifts in the mussel shells of Lake Balaton, the negative $\delta^{13}C$ and $\delta^{18}O$ shifts in the Renella and the Corchia cave records, the $\delta^{18}O$ peak in the COMNISPA II record, the sudden decrease of the Mg/Ca values in the Bunker Cave stalagmite and the Ti peak in the Ighiel lake sediments (Fig. 8). Contemporaneously, the H isotope compositions and the calculated temperatures are shifted to elevated values (Fig. 8, top panel). As we have seen, the high calculated temperatures, well above 10°C, can be explained by a relative increase in summer precipitation or evaporatively modified composition of the seepage water. The same

conclusion for temperature rise can be drawn from the bone carbonate $\delta^{18}O$ values that have their maximum in this period (Fig. 5).

The carbon isotope compositions of the Trió and the Sofular stalagmites indicate a short-term increase (along with P concentration decrease in the Trió stalagmite) between 3.65 and 3.5 cal ka BP (Figs. 5 and 8) that might be related to an environmental deterioration event (Siklósy et al., 2009) related to the Thera eruption (Manning et al., 2006). In addition to this local effect, precipitation level and/or temperature were continuously changing as indicated by the decreasing Mg concentrations and $\delta^{18}O$ values (temperature change) and the increased P contents (humidity change) in the Trió stalagmite, the fluctuating, but rising $\delta^{13}C$ values of the Corchia stalagmite and the decreasing Bunker Cave Mg/Ca record (Fig. 8). Although not plotted in Fig. 8 due to the low sampling resolution (~50 years), it is important to note that the $\delta^{18}O$ record for Lake Shkodra (Montenegro and Albania, Zanchetta et al., 2012) indicates short-term dry periods around 3.5 and 3.3 cal ka BP that are close (within dating precision) to the positive $\delta^{13}C$ peaks in the Trió record.

The Trió Mg concentrations and $\delta^{18}O$ values (Fig. 5), the Renella and Corchia records and the Bunker Cave Mg/Ca data show a distinct negative peak between 3.4 and 3.5 cal ka BP (Fig. 8), indicating a regionally important climate event. The Trió $\delta^{13}C$ values are still low compared to the subsequent period of 3.2 to 3.0 cal ka BP, but slightly higher than in the period of 3.7 to 3.6 cal ka BP, suggesting that the changes are not simply caused by increasing annual precipitation level. The calculated temperatures for the Trió stalagmite reach a minimum around 3.3-3.6 cal ka BP that practically covers the low $\delta^{18}O$ peak due to the δD sampling resolution (about ±50 years). The unrealistically low temperature (<0 °C, i.e., freezing in the cave) is most probably related to a bias in the δD values towards winter precipitation dominance (see above). All this information indicates elevated precipitation

with an increased winter/summer ratio for the period of 3.5 to 3.4 cal ka BP, with the possibility of cooling in the region of the Trió Cave, as summarized in the top panel of Fig. 8.

Following the humidity peak, the environmental parameters changed to warmer and drier conditions, as indicated by the constant rising of the Mg content, carbon and oxygen isotope compositions of the Trió, the Corchia, the Bunker and the Sofular Cave's stalagmites.

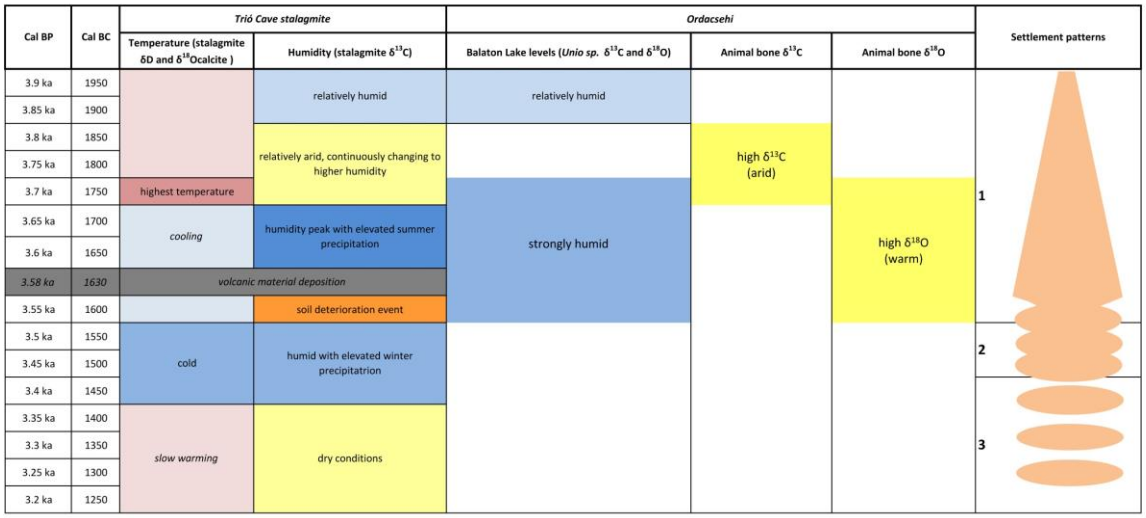

Fig. 9. Comparison of paleoclimate and archaeological information gathered for the period of cca. 3.9 to 3.2 cal ka BP (1950 to 1250 cal BC). See text for further details.

6.4. Societal changes related to environmental conditions

Screening the currently available archaeological information from the Pannonian Basin for the period of about 4 to 3 cal ka BP (see section 2), the only societal change that can be related to climate conditions is changes in settlement patterns. One of the major features of the Middle Bronze Age in this territory is the formation of the so-called 'tell' or stratified settlements. An increased number and size of settlements during the MBA, inferred from the archaeological evidence, was interpreted as an indication of demographic

growth (Chapman, 1999; Szeverényi, 2004; Kiss, 2012; Fischl et al., 2013), lasting until the short-lived (~150 years) Koszider period around 3.5 cal ka BP. Then, the tell settlements were replaced by a more open habitation type and a strong population decrease can be assumed, although it should be mentioned that these did not take place equally in the entire Pannonian Basin (see section 2). The associated cultural transition was related to the Tumulus culture, which is characterized by sporadically occurring open settlements, indicating decreased population compared to the early part of the MBA.

These settlement pattern variations can be partially explained by the reconstructed paleoclimate changes. In a comprehensive review, Fischl et al. (2013) summarized current knowledge on environmental effects on societal changes that can be compared with the climate conditions inferred from the speleothem and shell compositions (Fig. 9). The period between ~4 and 3.5 cal ka BP is characterized by fluctuating humidity but a relatively warm climate that provided appropriate conditions for agriculture and demographic growth. These environmental conditions ended with strong cooling associated with an increase in winter precipitation that may have contributed to the sudden drop in population size.

The Koszider period (~3.55-3.45 cal ka BP, see Fischl et al., 2013) is practically (within dating precision) coeval with the Thera eruption in Santorini that caused significant cultural collapse in the Eastern Mediterranean. The effects of the Thera eruption have been detected in the stable isotope and trace element compositions of the Trió speleothem (Siklósy et al., 2009). The short-lived environmental deterioration and the decrease in soil activity is reflected by the positive $\delta^{13}C$ and negative P concentration peaks in the Trió speleothem record (Fig. 5) at 3580 ±10 cal years BP. The suddenly deteriorating environmental conditions most probably contributed to the demographic decrease inferred for the Koszider period.

After the first phase of the LBA (~3.2 cal ka BP), climate conditions became drier and warmer (Fig. 9), but the number of settlements in all the above-mentioned regions was still lower than in the MBA. The dry/warm peak at about 3.2 cal ka BP (indicated by the positive $\delta^{13}C$, $\delta^{18}O$ and temperature peaks in the Trió speleothem record, Fig. 5) has also been observed in the Mediterranean region as a severe societal collapse (Drake, 2012; Langgut et al., 2015; Knapp and Manning, 2016), suggesting that the detected overall fall in the number of sites in the Tumulus period in the Pannonian Basin (V. Szabó, 1999; Sánta, 2010, 2012) can be partly related to environmental deterioration.

Although a comparison with other studies on climate-society relationships in the European-Mediterranean region seems to be a straightforward step, the results of such comparisons are rather questionable. As Knapp and Manning (2016) pointed out, the changes are too complex and the observations are sometimes contradictory, even within the Mediterranean region. Opposing climate changes have been detected for the same periods in northern and southern parts of the Alps (Valsecchi et al., 2006; Tinner et al., 2003), and similarly negative relationships appear if the Trió speleothem record is compared with Bronze Age water levels in Ireland (Amesbury et al., 2008), which suggest cold and humid conditions around 3.3 to 3.1 cal ka BP, when the Trió record indicates a warm and dry climate. The solution is the highly mosaic environmental pattern in the European-Mediterranean region that is convincingly demonstrated by the millennial temperature and precipitation map series of Mauri et al. (2015). The evaluation of the complex and temporally varying picture of climate conditions, and their effects on societal transitions, requires further, large scale studies.

6. Conclusions

The hydrogen isotope composition of fluid inclusion hosted waters from a stalagmite from the Trió Cave, Southern Hungary were obtained by vacuum crushing and isotope ratio mass spectrometry. Together with the published oxygen isotope composition of the host calcite, the H isotope data were used to calculate water composition and past formation temperatures for the period from 3 to 4 cal ka BP. In addition to temperature variations, humidity changes were inferred from coupled fluctuations in stable carbon isotope composition and P concentrations.

As independent proxies for temperature and precipitation, stable C and O isotope data were obtained for lake dwelling bivalve shells and animal bones collected from archaeological excavations of the Bronze Age (about 3 to 4 cal ka BP) at Lake Balaton (Western Hungary). A combined evaluation of the various proxy data and their comparison with other high-resolution paleoclimate records resulted in a complex climate evolution scheme, including temperature, humidity and seasonality changes on a regional scale. The environmental variations were associated with societal changes in the same period, among which, settlement pattern changes seem to best reflect climate conditions.

Acknowledgements

The study was financially supported by the Hungarian Scientific Research Fund (OTKA K-68343, T 049713) and the National Research, Development and Innovation Office (OTKA 101664). Precipitation monitoring was conducted in the framework of the project SNN 118205 financed by the National Research, Development and Innovation Office. The paper greatly benefited from detailed and helpful reviews from two anonymous reviewers that are gratefully acknowledged.

References

Amesbury, M.J., Charman, D.J., Fyfe, R.F., Langdon, P.G., West, S., 2008. Bronze Age upland settlement decline in southwest England: testing the climate change hypothesis. Journal of Archaeological Science 35, 87–98.

Amiot, R., Wang, X., Lécuyer, C., Buffetaut, E., Boudad, L., Cavin, L., Ding, Z., Fluteau, F., Kellner, A.W.A., Tong, H., Zhang, F., 2010. Oxygen and carbon isotope compositions of middle Cretaceous vertebrates from North Africa and Brazil: ecological and environmental significance. Palaeogeogr. Palaeoclimatol. Palaeoecol. 297, 439–451.

Armit, I., Swindles, G.T., Becker, K., Plunkett,G., Blaauw, M. (2014): Rapid climate change did not cause population collapse at the end of the European Bronze Age. PNAS, 111, 17045–17049.

Barbin, V. 2013. Application of cathodoluminescence microscopy to recent and past biological materials: a decade of progress. Miner. Petrol. 107, 353–362.

Boch, R., Spötl, C., Frisia, S., 2011. Origin and palaeoenvironmental significance of lamination in stalagmites from Katerloch Cave, Austria. Sedimentology 58, 508–531.

Bóna, I., 1992. Bronzezeitliche Tell-Kulturen in Ungarn. In: Meier-Arendt, W. (Ed.), Bronzezeit in Ungarn. Forschungen in Tell-Siedlungen an Donau und Theiß. Ausstellungskatalog. Museum für Vor- und Frühgeschichte, Archäologisches Museum, Frankfurt am Main, pp. 9–39.

Bondár, M., 1996. Early Bronze Age settlement patterns in South-West Transdanubia. Antaeus 22, 197–268.

Borsato, A., Frisia, S., Fairchild, I. J., Somogyi, A., Susini, J., 2007. Trace element distribution in annual stalagmite laminae mapped by micrometer-resolution X-ray fluorescence: implications for incorporation of environmentally significant species. Geochimica et Cosmochimica Acta 71, 1494–1512.

Borsato, A., Johnston, V.E., Frisia, S., Miorandi, R., Corradini, F., 2016. Temperature and altitudinal influence on karst dripwater chemistry: Implications for regional-scale palaeoclimate reconstructions from speleothems. Geochimica et Cosmochimica Acta 177, 275–297.

Bösel, M., 2008. Wandel durch Bronze? – Vergleichende Untersuchung sozialer Strukturen auf früh- und mittelbronzezeitlichen Gräberfeldern im Theißgebiet. Prähistorische Zeitschrift 83, 45–108.

Bronk Ramsey, C., 2001. Development of the radiocarbon calibration program OxCal. Radiocarbon 43, 355–363.

Carroll, M., Romanek, Ch.S., 2008. Shell layer variation in trace element concentration for the freshwater bivalve. Elliptio complanata: Geo-Marine Letters 28, 369–381.

Chapman, J., 1999. Burning the ancestors: deliberate housefiring in Balkan prehistory. In: Gustafsson, A., Karlsson, H. (Eds.), Glyfer och arkeologiska rum – en vänbok till Jarl Nordbladh. Gotarc Series A, vol. 3. University of Gothenburg, Department of Archaeology, Göteborg, pp. 113–126.

Choyke, A. M., Bartosiewicz, L., 2000. Bronze Age animal exploitation on the Central Great Hungarian Plain. Acta Archaeologica Academiae Scientiarum Hungaricae 51, 43–70.

Clark, I. D. and Fritz, P., 1997. Environmental Isotopes in Hydrogeology. Lewis Publishers, New York, 328 pp.

Coplen, T.B., 2007. Calibration of the calcite-water oxygen-isotope geothermometer at Devils Hole, Nevada, a natural laboratory. Geochim. Cosmochim. Acta 71, 3948–3957.

Craig H., 1961. Isotopic variations in meteoric waters. Science 133, 1702–1703.

Csányi, M., 2003. The Tumulus culture: invaders from the west. In: Visy, Zs. (Ed.), Hungarian Archeology at the Turn of the Millennium. Ministry of National Cultural Heritage, Budapest, 161–163.

Czuppon, Gy., Demény, A., Leél-Őssy, Sz., Óvari, M., Molnár, M., Stieber, J., Kiss, K., Kármán, K., Surányi, G., Haszpra, L., 2017. Cave monitoring in the Béke and Baradla Caves (Northeastern Hungary): implications for the conditions for the formation cave carbonates. International Journal of Speleology (in press).

Dansgaard, W., 1964. Stable isotopes in precipitation. Tellus 16, 436–468.

Demény, A., 1995. H isotope fractionation due to hydrogen– zinc reactions and its implications on D/H analysis of water samples. Chem. Geol. 121, 19–25.

Demény, A., Siklósy, Z., 2008. Combination of off-line preparation and continuous flow mass spectrometry: D/H analyses of inclusion waters. Rapid Commun. Mass Spectrom. 22, 1329–1334.

Demény, A., Németh, A., Kern, Z., Czuppon, Gy., Molnár, M., Leél-Őssy, Sz., Óvári, M., Stieber, J., 2017a. Recently forming stalagmites from the Baradla Cave and their suitability assessment for climate-proxy relationships. Central European Geology 60, 1–34.

Demény, A., Kern, Z., Czuppon, Gy., Németh, A., Leél-Őssy, Sz., Siklósy, Z., Lin, K., Hsun-Ming, H., Shen, Ch-Ch., Vennemann, T .W., Haszpra, L., 2017b. Stable isotope compositions of speleothems from the last interglacial – Spatial patterns of climate fluctuations in Europe. Quaternary Science Reviews 161, 68–80.

Dettman, D.L., Reische, A.K., Lohmann, K. C., 1999. Controls on the stable isotope composition of seasonal growth bands in aragonitic fresh-water bivalves (Unionidae). Geochim. Cosmochim. Acta 63, 1049–1057.

Dorale, J.A., Liu, Z., 2009. Limitations of Hendy test criteria in judging the paleoclimatic suitability of speleothems and the need for replication. J. Caves Karst Stud. 71, 73–80.

Drake, B.L. (2012): The influence of climatic change on the Late Bronze Age Collapse and the Greek Dark Ages. Journal of Archaeological Science 39, 1862–1870.

Drysdale, R.N., Zanchetta, G., Hellstrom, J.C., Maas, R., Fallick, A.E., Pickett, M., Cartwright, I., Piccini, L., 2006. Late Holocene drought responsible for the collapse of Old World civilizations is recorded in an Italian cave flowstone. Geology 34, 101–104.

Earle, R., Kolb, M. J., 2010. Regional Settlement Patterns. In: Earle, T., Kristiansen, K. (Eds.), Organizing Bronze Age Societies. The Mediterranean, Central Europe, and Scandinavia Compared. Cambridge University Press, Cambridge, 57–86.

Fairchild, I.J., Baker, A., 2012. Speleothem Science. Wiley-Blackwell, 450 pp.

Fairchild, I.J., Baker , A., Borsato, A., Frisia, S., Hinton, R.W., McDermott, F., Tooth, A.F., 2001. Annual to sub -annual resolution of multiple trace element trends in speleothems. J. Geol. Soc. 158, 831–841.

Fairchild, I. J., Smith, C. L., Baker, A., Fuller, L., Spötl, C., Mattey, D., McDermott, F., E. I. M. F., 2006. Modification and preservation of environmental signals in speleothems. Earth-Science Reviews 75, 105–153.

Finné, M., Holmgren, K., Sundqvist, H. S., Weiberg, E., & Lindblom, M. (2011). Climate in the eastern Mediterranean, and adjacent regions, during the past 6000 years–A review. Journal of Archaeological Science 38, 3153–3173.

Fischl, K. P., Kiss, V., Kulcsár, G., Szeverényi, V., 2013. Transformations in the Carpathian Basin around 1600 B. C. In: Meller, H., Bertemes, F., Bork, H.-R., Risch, R. (Eds.), 1600

– Cultural change in the shadow of the Thera-Eruption? Tagungen des Landesmuseums für Vorgeschichte Halle (9). Landesamt für Denkmalpflege und Archäologie Sachsen-Anhalt – Landesmuseum für Vorgeschichte, Halle, pp. 355–372.

Fleitmann, D., Cheng, H., Badertscher, S., Edwards, R. L., Mudelsee, M., Göktürk, O. M., Fankhauser, A., Pickering, R., Raible, C. C., Matter, A., Kramers, J., Tüysüz, O., 2009. Timing and climatic impact of Greenland interstadials recorded in stalagmites from northern Turkey. Geophys. Res. Lett. 36, L19707.

Fohlmeister, J., Schröder-Ritzrau, A., Spötl, C., Frisia, S., Miorandi, R., Kromer, B., Mangini, A., 2010. The influences of hydrology on the radiogenic and stable carbon isotope composition of cave drip water, Grotta di Ernesto (Italy). Radiocarbon 52, 1529–1544.

Fohlmeister, J., Schröder-Ritzrau, A., Scholz, D., Spötl, C., Riechelmann, D., Mudelsee, M., Wackerbarth, A., Gerdes, A., Riechelmann, S., Immenhauser, A., Richter, D., Mangini, A., 2012. Bunker cave stalagmites: An archive for central European Holocene climate variability. Clim. Past 8 , 1751–1764.

Fohlmeister, J., Vollweiler, N., Spötl, C., Mangini, A., 2013. COMNISPA II: update of a mid-European isotope climate record, 11 ka to present. The Holocene 23, 749–754.

Fórizs, I., 2005. Processes behind the isotopic water line: water cycle and climate. Studia Universitatis Babeş-Bolyai, Physica L, 138-146.

Fórizs, I., Csicsák, J., Ország, J., Vendégh, R., Kern, Z., 2013. Environmental isotopes in precipitation, Mecsek Mts, Hungary (Presentation). Presented at: ESIR XII – Workshop, 24–26 July: 2013: Isotopes in Earth Systems - Freiberg, TU Bergakademie Freiberg.

Freeman, S. P. H. T., Cook, G. T., Dougans, A. B., Naysmith, P., Wilcken, K. M., Xu S., 2010. Improved SSAMS performance. Nuclear Instruments and Methods B 268, 715–717.

Frisia S., Borsato A., 2010. Karst. Developments in Sedimentology, Chapter 6, 61, 269–318.

Frisia, S., Borsato, A., Fairchild, I.J., McDermott, F., 2000. Calcite fabrics, growth mechanisms and environments of formation in speleothems from the Italian Alps and southwestern Ireland. Journal of Sedimentary Research 70, 1183–1196.

Frisia, S., Borsato, A., Spötl, C., Villa, I.M., Cucchi, F., 2005. Climate variability in the SE Alps of Italy over the past 17000 years reconstructed from a stalagmite record. Boreas 34, 445–455.

Gogâltan, F., 2002. Die Tells der Bronzezeit im Karpatenbecken. Terminologische Fragen. In: Rustoiu, A., Ursuţiu, A. (Eds.), Interregionale und Kulturelle Beziehungen im Karpatenraum (2. Jahrtausend v. Chr.–1. Jahrtausend n. Chr.). Interferenţe etnice şi culturale în mileniile I a. Chr.–I. p. Chr. Ethnische und kulturelle Interferenzen im 1. Jahrtausend v. Chr.–1. Jahrtausend n. Chr. 4. Nereamia Napocae, Cluj-Napoca, pp. 11–45.

Griffiths, M.L., Fohlmeister, J., Drysdale, R.N., Hua, Q., Johnson, K.R., Hellstrom, J.C., Gagan, M.K., Zhao, J.-X., 2012. Hydrological control of the dead carbon fraction in a Holocene tropical speleothem. Quaternary Geochronology 14, 81–93.

Guiot, J., Kaniewski, D., 2015. The Mediterranean Basin and Southern Europe in a warmer world: what can we learn from the past? Front. Earth Sci. 3, Art. 28.

Gyulai, F., 2010. Fruit, Food and Beverage Remains in the Carpathian Basin from the Neolithic to the Late Middle Ages. Archaeolingua 21, Budapest.

Hajdu, T., 2012. A bronzkori Füzesabony- és Halomsíros kultúra népességének biológiai rekonstrukciója [Biological reconstruction of the population of the Bronze Age Füzesabony and Tumulus Grave cultures]. Unpubl. PhD Thesis. Budapest.

Haliuc, A., Veres, D., Brauer, A., Hubay, K., Hutchinson, S. M., Begy, R., Braun, M., 2017. Palaeohydrological changes during the mid and late Holocene in the Carpathian area, central-eastern Europe. Glob. Planet. Change 152, 99–114.

Hammer, Ø., Harper, D.A.T., Ryan, P. D., 2001. PAST: Paleontological Statistics Software Package for Education and Data Analysis. Palaeontologia Electronica 4, pp. 9.

Harding, A. F., 2000. European Societies in the Bronze Age. Cambridge University Press, Cambridge.

Harmon, R. S., Schwarcz H. P., O'Neil J. R., 1978. D/H ratios in speleothem fluid inclusions: a guide to variations in the isotopic composition of meteoric precipitation? Earth Planet. Sci. Lett. 42, 254–266.

Hendy, C. H., 1971. The isotopic geochemistry of speleothems: I. The calculation of the effects of different modes of formation on the isotopic composition of speleothems and their applicability as palaeoclimatic indicators. Geochim. Cosmochim. Acta 35, 801–824.

Huang, Y., Fairchild, I. J., 2001. Partitioning of Sr^{2+} and Mg^{2+} into calcite under karst-analogue experimental conditions. Geochimica et Cosmochimica Acta 65, 47–62.

Huang, Y. , Fairchild, I.J., Borsato, A., Frisia, S., Cassidy, N.J., McDermott, F., Hawkesworth, C.J., 2001. Seasonal variations in Sr, Mg and P in modern speleothems (Grotta di Ernesto, Italy) . Chem. Geol. 175, 429–448.

Johnston, V.E., Borsato, A., Spötl, C., Frisia, S., Miorandi, R., 2013. Stable isotopes in caves over altitudinal gradients: fractionation behaviour and inferences for speleothem sensitivity to climate change. Clim. Past 9, 99–118.

Kiss, A. 2009. Historical climatology in Hungary: Role of documentary evidence in the study of past climates and hydrometeorological extremes. Időjárás 113, 315–339.

Kiss, V., 2012. Middle Bronze Age Encrusted Pottery in western Hungary. Varia Archaeologica Hungarica 27. Arcaheolingua, Budapest.

Kiss, V., Belényesy, K., Honthi Sz., 2007. Rolling time. Excavations on the M7 Motorway in County Somogy between Zamárdi and Ordacsehi. Archaeological Institute, Budapest. pp. 351.

Kiss, A., Laszlovszky, J., 2013. 14th-16th-century Danube floods and long-term water-level changes in archaeological and sedimentary evidence in the western and central Carpathian Basin: An overview with documentary comparison. Journal of Environmental Geography 6, 1–11.

Kiss, A., Nikolić, Z., 2015. Droughts, Dry Spells and Low Water Levels in Medieval Hungary (and Croatia) I: The Great Droughts of 1362, 1474, 1479, 1494 and 1507. Journal of Environmental Geography 8, 11–22.

Koch, P. L., Tuross, N., Fogel, M. L., 1997. The effects of sample treatment and diagenesis on the isotopic integrity of carbonate in biogenic hydroxylapatite. J. Archaeol. Sci. 24, 417–429.

Koltai, G., Kele, S., Surányi, G., Muladi, B., Bárány-Kevei, I., 2013. Preliminary results on paleoclimate research in Mecsek Mts, Hungary. In: 16th International Congress of Speleology. Czech Speleological Society, Prague, pp. 423–426.

Knapp, B.A., Manning, S.W., 2016. Crisis in Context: The End of the Late Bronze Age in the Eastern Mediterranean. American Journal of Archaeology 120, 99–149.

Krenn-Leeb, A., 2006. Gaben an die Götter? Depotfunde der Frühbronzezeit in Österreich. Archäologie Österreichs 17, 4–17.
Kulcsár, G., 2009. The Beginnings of the Bronze Age in the Carpathian Basin. The Makó–Kosihy–Čaka and the Somogyvár–Vinkovci cultures in Hungary. Varia Archaeologica Hungarica 23, Budapest.
Kulcsár, G., Szeverényi, V., 2013. Transition to the Bronze Age: Issues of Continuity and Discontinuity in the First Half of the Third Millennium BC in the Carpathian Basin. In: Heyd, V., Kulcsár, G., Szeverényi, V. (Eds.), Transitions to the Bronze Age. Interregional Interaction and Socio–Cultural Changes in the Tird Millennium BC Carpathian Basin and Neighbouring Regions. Archaeolingua, Budapest, pp. 67–92.
Lachniet, M. S., 2009. Climatic and environmental controls on speleothem oxygen-isotope values. Quat. Sci. Rev. 28, 412–432.
Lamb, H.H., 1982. Climate, History and the Modern World. Methuen, London, p. 433.
Langgut, D., Finkelstein, I., Litt, T., Neumann, F.H., Stein, M., 2015. Vegetation and Climate Changes during the Bronze and Iron Ages (~3600–600 BCE) in the Southern Levant Based on Palynological Records. Radiocarbon 57, 217–235.
Lee-Thorp, J., 2002. Two decades of progress towards understanding fossilization processes and isotopic signals in calcified tissue minerals. Archaeometry 44, 435–446.
Longinelli, A., 1984. Oxygen isotopes in mammal bone phosphate: a new tool for paleohydrological and paleoclimatological research? Geochim. Cosmochim. Acta 48, 385–390.
Luz, B., Kolodny, Y., 1985. Oxygen isotope variations in phosphate of biogenic apatites, IV. Mammal teeth and bones. Earth Planet. Sci. Lett. 75, 29–36.
Mangini, A., Verdes, P., Spötl, C., Scholz, D., Vollweiler, N., Kromer, B., 2007. Persistent influence of the North Atlantic hydrography on central European winter temperature during the last 9000 years. Geophys. Res. Lett. 34, L02704.
Manning, S.W., Ramsey, C.B., Kutschera, W., Higham, T., Kromer, B., Steier, P., Wild, E.M., 2006. Chronology for the Aegean Late Bronze Age 1700-1400 B.C. Science 312, 565–569.
Mauri, A., Davis, B.A.S., Collins, P.M., Kaplan, J.O., 2016. The climate of Europe during the Holocene: a gridded pollen-based reconstruction and its multi-proxy evaluation. Quaternary Science Reviews 112, 109–127.
Mayewski, P.A., Rohling, E.E., Stager, J.C., Karlen, W., Maasch, K.A., Meeker, L.D., Meyerson, E.A., Gasse, F., van Kreveld, S., Holmgren, K., Lee-Thorp, J., Rosqvist, G. Rack, F., Staubwasser, M., Schneider, R.R., Steig, E.J., 2004. Holocene climate variability. Quaternary Research 62, 243–255.
Meller, H., Bertemes, F., Bork, H.-R., Risch, R. (Eds.), 2013. 1600 BC – Cultural change in the shadow of the Thera-Eruption? Tagungen des Landesmuseums für Vorgeschichte Halle (9). Landesamt für Denkmalpflege und Archäologie Sachsen-Anhalt – Landesmuseum für Vorgeschichte, Halle
Menotti, F., 2009. Climate variations in the Circum-Alpine region and their influence on Neolithic-Bronze Age lacustrine communities: Displacement and/or cultural adaptation. Documenta Praehistorica, 36, 61–66.
Mensing, S. A., Tunno, I., Sagnotti, L., Florindo, F., Noble, P., Archer, C., Zimmermann, S., Pavón-Carrasco, F., Cifani, G., Passigli, S., Piovesan, G., 2015. 2700 years of Mediterranean environmental change in central Italy: a synthesis of sedimentary and

cultural records to interpret past impacts of climate on society. Quaternary Science Reviews, 116, 72–94.
Mickler, P. J., Stern, L. A., Banner, J. L., 2006. Large kinetic isotope effects in modern speleothems. GSA Bulletin 118, 65–81.
Mickler, P. J., Banner, J. L., Stern, L., Asmerom, Y., Edwards, R.L., Ito E., 2004. Stable isotope variations in modern tropical speleothems: evaluating equilibrium vs. kinetic effects. Geochim. Cosmochim. Acta 68, 4381–4393.
Muladi, B., Csépe, Z., Mucsi, L., Puskás, I., Koltai, G., Bauer, M., 2013. Climatic features of different karst caves in Hungary In: Michal Filippi, Pavel Bosák (szerk.) 16th International Congress of Speleology: Proceedings Volume 2 Prague: Czech Speleological Society, 432–438.
Nagy, G., 1968. Triassic formations of the Mecsek Mts. Annual Report of the Hungarian Geological Institute LI, pp. 198.
Neugebauer, J.-W., 1994. Bronzezeit in Ostösterreich. Forschungsberichte zur Ur- und Frühgeschichte 16. Niederösterreichisches Pressehaus, St. Pölten, Wien.
Noronha, A.L., Johnson, K.R., Hu, C., Ruan, J., Southon, J.R., Ferguson, J.E., 2014. Assessing influences on speleothem dead carbon variability over the Holocene: implications for speleothem-based radiocarbon calibration. Earth and Planetary Science Letters 394, 20–29.
O'Neil, J.R., Clayton, R., Mayeda, T., 1969. Oxygen isotopic fractionation in divalent metal carbonates. J. Chem. Phys. 51, 5547–5558.
O'Shea, J., 2011. A River Runs Through It: Landscape and the Evolution of Bronze Age Networks in the Carpathian Basin. Journal World Prehistory 24, 161–174.
Peyron, O., Combourieu-Nebout, N., Brayshaw, D., Goring, S., Andrieu-Ponel, V., Desprat, S., Fletcher, W., Gambin, B., Ioakim, C., Joannin, S., Kotthoff, U., Kouli, K., Montade, V., Pross, J., Sadori, L., Magny, M., 2017. Precipitation changes in the Mediterranean basin during the Holocene from terrestrial and marine pollen records: a model–data comparison, Clim. Past, 13, 249–265.
Pinke, Z., Ferenczi, L., Gábris, G., Nagy, B. 2016. Settlement patterns as indicators of water level rising? Case study on the wetlands of the Great Hungarian Plain. Quaternary International 415, 204–215
Pinke, Z., Ferenczi, L., Romhányi, B. F., Gyulai, F., Laszlovszky, J., Mravcsik, Z., Pósa, P., Gábris, G., 2017. Zonal assessment of environmental driven settlement abandonment in the Trans-Tisza region (Central Europe) during the early phase of the Little Ice Age. Quaternary Science Reviews 157, 98–113
Primavera, M., D'Oronzo, C., Muntoni, I.M., Radina, F., Fiorentino, G., 2017. Environment, crops and harvesting strategies during the II millennium BC: Resilience and adaptation in socio-economic systems of Bronze Age communities in Apulia (SE Italy). Quaternary International 436, 83–95.
Regattieri, E., Zanchetta, G., Drysdale, R.N., Isola, I., Hellstrom, J.C., Dallai, L., 2014. Lateglacial to Holocene trace element record (Ba, Mg, Sr) from Corchia Cave (Apuan Alps, central Italy): paleoenvironmental implications. Journal of Quaternary Science 29, 381–392.
Regattieri, E., Zanchetta, G., Drysdale, R. N., Isola, I., Woodhead, J. D., Hellstrom, J. C., Giaccio, B., Greig, A., Baneschi, I., Dotsika, E., 2016. Environmental variability between the penultimate deglaciation and the mid Eemian: Insights from Tana che

Urla (central Italy) speleothem trace element record. Quaternary Science Reviews, 152, 80–92.
Reimer, P.J., Bard, E., Bayliss, A., Beck, J.W., Blackwell, P.G., Bronk Ramsey, C., Grootes, P.M., Guilderson, T.P., Haflidason, H., Hajdas, I., Hatte, C., Heaton, T.J., Hoffmann, D.L., Hogg, A.G., Hughen, K.A., Kaiser, K.F., Kromer, B., Manning, S.W., Niu, M., Reimer, R.W., Richards, D.A., Scott, E.M., Southon, J.R., Staff, R.A., Turney, C.S.M., van der Plicht, J., 2013. IntCal13 and Marine13 radiocarbon age calibration curves 0-50,000 years cal BP. Radiocarbon 55, 1869–1887.
Reményi, L., 2009. A nagyrévi kultúra kulturális és kronológiai kérdései (Cultural and chronological Questions of Nagyrév culture). Tisicum: a Jász-Nagykun-Szolnok megyei múzeumok évkönyve XIX, pp. 229–254.
Rozanski, K., Araguas-Araguas, L., Gonfiantini, R., 1993. Isotopic patterns in modern global precipitation. Geophysical Monograph 78, 1–36.
Sánta, G., 2010. Settlements of the Tumulus Culture in Hungary. Antaeus 31–32, 513–528.
Sánta, G., 2012. Domaszék-Börcsök tanya (Halomsíros település) komplex, régészeti, környezetrégészeti és archaeometriai elemzése [Complex archaeological, environmental archaeological and archaeometric analysis of Domaszék-Börcsök Tanya (Tumulus settlement)]. Unpubl. PhD Thesis. Szeged.
Scholz, D., Hoffmann, D.L., 2011. StalAge - an algorithm especially designed for construction of speleothem age. Quaternary Geochronology 6, 369–382.
Schöll-Barna, G., 2011. An isotope mass balance model for the correlation of freshwater bivalve shell (Unio pictorum) carbonate $\delta^{18}O$ to climatic conditions and water $\delta^{18}O$ in Lake Balaton (Hungary). Journal of Limnology 70, 272–282.
Schöll-Barna, G., Demény, A., Serlegi, G., Fábián, S., Sümegi, P., Fórizs, I., Bajnóczi B., 2012. Climatic variability in the Late Copper Age: Stable isotope fluctuation of prehistoric Unio pictorum (Unionidae) shells from Lake Balaton (Hungary). Journal of Paleolimnology 47, 87–100.
Schöne, B. R., Fiebig J., 2009. Seasonality in the North Sea during the Allerød and Late Medieval Climate Optimum using bivalve sclerochronology. Int. J. Earth Sci. (Geol. Rundsch.) 98, 83–98.
Schwarcz, H. P., Harmon, R. S., Thompson, P., Ford D. C., 1976. Stable isotope studies of fluid inclusions in speleothems and their paleoclimatic significance. Geochim. Cosmochim. Acta 40, 657–665.
Siklósy, Z., Demény, A., Vennemann, T. W., Pilet, S., Kramers, J., Leél-Őssy, Sz., Bondár, M., Shen, C.-C., Hegner E., 2009. Bronze Age volcanic event recorded in stalagmites by combined isotope and trace element studies. Rapid Commun. Mass Spectrom. 23, 801–808.
Slota, Jr. P. J., Jull, A. J. T., Linick, T. W., Toolin L. J., 1987. Preparation of small samples for ^{14}C accelerator targets by catalytic reduction of CO. Radiocarbon 29, 303–306.
Spötl, C., Vennemann, T. W., 2003. Continuous−flow isotope ratio mass spectrometric analysis of carbonate minerals. Rapid Commun. Mass Spectrom. 17, 1004–1006.
Szeverényi, V., 2004. The Early and Middle Bronze Ages in Central Europe. In: Bogucki, P., Crabtree, P. J. (Eds.), Ancient Europe 8000 B. C.–A. D. 1000. Encyclopedia of the Barbarian World. Vol. II: Bronze Age to Early Middle Ages (c. 3000 B. C.–A. D. 1000). Charles Scribner's Sons, New York, pp. 20–30.

Tinner, W., Lotter, A.F., Ammann, B., Conedera, M., Hubschmid, P., van Leeuwen, J.F.N., Wherli, M., 2003. Climatic change and contemporaneous land-use phases north and south of the Alps 2300 BC to 800 AD. Quaternary Science Reviews 22, 1447–1460.

Tremaine, D.M., Froelich, P.N., Wang, Y., 2011. Speleothem calcite farmed in situ: Modern calibration of $\delta^{18}O$ and $\delta^{13}C$ paleoclimate proxies in a continuously-monitored natural cave system. Geochim. Cosmochim. Acta 75**,** 4929–4950.

Treble, P., Shelley, J.M.G., Chappell, J., 2003. Comparison of high resolution subannual records of trace elements in a modern (1911–1992) speleothem with instrumental climate data from southwest Australia. Earth and Planetary Science Letters 216, 41–153.

Türkes, M., Erlat, E., 2003. Precipitation changes and variability in Turkey linked to the North Atlantic Oscillation during the period 1930-2000. International Journal of Climatology 23, 1771–1796.

V. Szabó, G., 1999. A bronzkor Csongrád megyében (Történeti vázlat a készülő állandó régészeti kiállítás kapcsán) (The Bronze Age in county Csongrád (A historical outline made on the occasion of the arrangement of the permanent archaeological exhibition). Múzeumi Füzetek (Csongrád) 2, pp. 51–118.

Vadas, A., 2013. The “waters leave their beds frequently”: a Western-Hungarian town and the flooding of the Rába/Raab River in the seventeenth century (1600–1658). Water History 5, 267–286

Vadas, A., Rácz, L. 2013. Climatic changes in the Carpathian Basin during the Middle Ages:The State of Research. Global Environment. 12. 198–227

Valsecchi, V., Tinner, W., Finsinger, W., Ammann, B., 2006 Human impact during the Bronze Age on the vegetation at Lago Lucone (northern Italy). Vegetation History and Archaeobotany 15, 99–113.

Vandeputte, K., Moens, L., Dams, R., 1996. Improved sealed-tube combustion of organic samples to CO_2 for stable carbon isotope analysis, radiocarbon dating and percent carbon determinations. Analytical Letters 29, 2761–2773.

Verdegaal, S., Troelstra, S.R., Beets, C.J., Vonhof, H.B., 2005. Stable isotopic records in unionid shells as a paleoenvironmental tool. Netherlands Journal of Geosciences 84, 403–408.

Versteegh, E. A. A., Troelstra, S. R., Vonhof, H. B., Kroon, D., 2009. Oxygen isotope composition of bivalve seasonal growth increments and ambient water in the rivers Rhine and Meuse. Palaios. 24, 497–504.

Visy, Zs., 2003. Hungarian Archaeology at the turn of the Millennium. Ministry of National Cultural Heritage, Budapest, pp. 487.

Vretemark, M., 2010. Subsistence Srategies. In: Earle, T., Kristiansen, K. (Eds.), Organizing Bronze Age Societies. The Mediterranean, Central Europe, and Scandinavia Compared. Cambridge University Press, Cambridge, pp. 155–184.

Wanner, H., Solomina, O., Grosjean, M., Ritz, S. P., Jetel, M., 2011. Structure and origin of Holocene cold events. Quaternary Science Reviews 30, 3109–3123.

Watkins, J.M., Hunt, J.D., Ryerson, F.J., DePaolo, D.J., 2014. The influence of temperature, pH, and growth rate on the $\delta^{18}O$ composition of inorganically precipitated calcite. Earth Planet. Sci. Lett. 404, 332–343.

Wróblewski, W., Gradziński, M., Motyka, J., Stankovič, J., 2017. Recently growing subaqueous flowstones: Occurrence, petrography and growth conditions. Quaternary International 437, 84–97.

Zanchetta, G., Van Welden, A., Baneschi, I., Drysdale, R., Sadori, L., Roberts, N., Giardini, M., Beck, C., Pascucci, V., Sulpizio, R., 2012. Multiproxy record for the last 4500 years from Lake Shkodra (Albania/Montenegro). Journal of Quaternary Science 27, 780–789.

Zanchetta, G., Regattieri, E., Isola, I., Drysdale, R.N., Bini, M., Baneschi, I., Hellstrom, J.C., 2016. The So-called "4.2 Event" in the central Mediterranean and its climatic teleconnections. Alpine and Mediterranean Quaternary 29, 5–17.

Zhang, R., Schwarcz, H. P., Ford, D. C., Serefiddin-Schroeder, F., Beddows, P. A., 2008. Absolute palaeotemperature record from 10 to 6 ka inferred from fluid inclusion D/H ratios of a stalagmite from Vancouver Island. British Columbia. Geochim. Cosmochim. Acta 72, 1014–1026.

Figure captions

Fig. 1. Locations of the archaeological site of Ordacsehi-Bugaszeg (bivalve shells) and the Trió Cave (stalagmite). Potential lake water levels are shown in C as heights above sea level.

Fig. 2. An age-depth model established from the original U/Th data of Siklósy et al. (2009) using the StalAge algorithm (Scholz and Hoffmann, 2011). The grey arrow marks the direction to the origin.

Fig. 3. AMS ^{14}C ages (A) and stable C and O isotope compositions (in ‰ relative to V-PDB) of carbonate contents of Unio *sp.* shells (B and C) and animal bones (D) collected from archaeological excavation sites of Ordacsehi-Bugaszeg (at Lake Balaton, Western Hungary).

Fig. 4. Carbonate fabrics occurring in the Trió core. (a) Porous columnar fabric with two orders of lamination (sub-laminae connected to thin detrital layers are aligned by blue arrows, while the macroscopically visible compact laminae are aligned by white arrows). (b) Compact columnar fabric with low porosity. (c) Microcrystalline fabric with interfingering extinction boundaries and high porosity. (d) Erosion surface in the lowermost section of the compact columnar fabric aligned by white arrow, covered by a series of brown laminae of detrital origin.

Fig. 5. Stable isotope compositions of shells and bones collected from archaeological excavations, H, C and O isotope compositions inclusion-hosted water and the host calcite along with P and Mg concentrations of the Trió stalagmite (Siklósy et al., 2009). Proxy records are arranged to reflect humidity (shell $\delta^{13}C$ and $\delta^{18}O$, Trió stalagmite P content and and $\delta^{13}C$) and temperature (Trió stalagmite δD, calculated temperatures, bone $\delta^{18}O$, Trió stalagmite Mg contents and $\delta^{18}O$). Calculated temperatures obtained by procedures 1 and 2 (see text) are shown by solid and dashed lines, respectively.

Fig. 6. Microstratigraphic log of the section between 200-360 mm from the top of Trió stalagmite along with stable C and O isotope compositions. Sections not covered with thin sections are marked by X. C: Dense columnar calcite (light blue). Co: porous columnar calcite (dark blue). Cm: Microcrystalline calcite, Ms: micrite/microsparite with high detrital content.

Fig. 7. Stable hydrogen isotope compositions (relative to V-SMOW) of inclusion-hosted water and oxygen isotope compositions of the host calcite (relative to V-PDB) at the inclusion sampling intervals of the Trió stalagmite. The grey line (arbitrarily placed within the sample points) marks slope=8 characteristic for the Global Meteoric Water Line (Craig, 1961).

Fig. 8. Temperature and precipitation proxy records for the Trió cave stalagmite (this study) and regional records. Data sources: Corchia cave (northern Italy): Regattieri et al. (2014); Renella cave (northern Italy): Zanchetta et al. (2016); Sofular Cave (northern Turkey): Fleitmann et al. (2009); Spannagel Cave (Austria): Fohlmeister et al. (2013); Bunker Cave (Germany): Fohlmeister et al. (2012); Lake Ighiel (Romania): Haliuc et al. (2017). Dark grey bars indicate humid phases, light grey bars mark dry periods.

Fig. 9. Comparison of paleoclimate and archaeological information gathered for the period of cca. 3.9 to 3.2 cal ka BP (1950 to 1250 cal BC). See text for further details.

Table 1

Archaeological cultures, animal species, types, stable carbon isotope compositions and AMS ^{14}C ages for bones of the Ordacsehi archaeological excavation sites. Ages are in years, $\delta^{13}C$ values are in ‰ relative to V-PDB. $\delta^{13}C$ values were determined by isotope ratio mass spectrometry, „AMS" means $\delta^{13}C$ values determined by AMS analyses for correction purpose (not to be reported).

Sample #	culture	animal species	bone type
1296/1880	Somogyvár-Vinkovci	bos taurus	centrotarsale
1882/2790	Kisapostag	bos taurus	radius
1309/1902	Late Kisapostag - Early encrusted pottery	bos taurus	mandibula
71/91	Encrusted Pottery	sus domesticus	radius/ulna
1325/1925	Tumulus	cervus elaphus	metatarsus

sample #	Lab code	$\delta^{13}C$	^{14}C age BP	age cal. BP (2σ range)	median	cal BC
1296/1880	SUERC-36668	–22.1	3615 ± 35	4071-4042 (5%) 3991-3837 (90.4%)	3925	1975
1882/2790	SUERC-36669	–20.0	3505 ± 35	3875-3691 (94.4%) 3658-3650 (1%)	3774	1824
1309/1902	VERA-5168	AMS	3535 ± 35	3905-3700	3814	1864
71/91	SUERC-36667	–20.5	3420 ± 35	3825-3790 (7.9%) 3770-3746 (3.5%) 3730-3576 (84%)	3669	1719
1325/1925	VERA-5167	AMS	3315 ± 40	3638–3453	3539	1589

Table 2

Stable hydrogen isotope compositions of fluid inclusion hosted water (δD), and oxygen isotope compositions of calcite of the Trió Cave ($\delta^{18}O_{Trió}$), Southern Hungary, and stable carbon and oxygen isotope compositions of *Unio* sp. shells and animal bones (see Table 1) collected at the archaeological excavation sites of Ordacsehi, Western Hungary. All data are in ‰ relative to V-SMOW (δD) or to V-PDB ($\delta^{13}C$ and $\delta^{18}O$). $\delta^{18}O$ values of stalagmite calcite ($\delta^{18}O_{Trió}$) are averages for the δD sampling sections calculated from the data reported by Siklósy et al. (2009). Shell compositions are averages for archaeological culture periods (see also Supplementary Table 1). Depth: distance from the outer surface of the stalagmite drill core.

Stalagmite data			Bones		
depth[mm]	δD	$\delta^{18}O_{Trió}$	sample #	$\delta^{13}C$	$\delta^{18}O$
337	–72	-7.2	1296/1880	–13.6	–6.8
292	–76	-7.4	1309/1902	–10.0	–5.0
276	–75	-7.1	1882/2790	–14.1	–4.4
272	–63	-6.6	71/91	–13.6	–3.3
259	–65	-8.3	1325/1925	–12.3	–5.4
254	–74	-7.8			
246	–90	-8.0			
241	–85	-8.8			
233	–86	-7.8			
222	–63	-6.1			
216	–74	-6.8			
209	–69	-7.5			
109	–68	-7.2			
66	–62	-7.7			

Shells							
Culture periods		$\delta^{13}C$			$\delta^{18}O$		
	median age	median	LQ	UQ	median	LQ	UQ
Somogyvár-Vinkovci	3925	-6.3	1.2	0.3	-3.9	1.2	0.3
Kisapostag	3774	-4.3	1.1	0.6	-1.8	0.4	0.8
Late Kisap. - Early encr.	3814	-4.5	0.4	0.5	-2.4	0.9	1.6
Encrusted Pottery	3669	-11.0	0.8	1.1	-7.9	0.1	0.3
Tumulus	3539	-4.7	0.4	0.4	-2.8	1.2	0.5